**Highlights:**

Review on single layer, dual layer and mixed matrix hollow fibres prepared by NIPS & TIPS techniques

Hollow fibre membranes are engineered for desalination by membrane distillation (MD)

The coagulant strength and the use of additives improve the MD membrane performance

Creation of aggregates limits the development of mixed matrix hollow fibre membranes

Delamination is a major problem in the production of dual layer hollow fibres

**Graphical abstract**

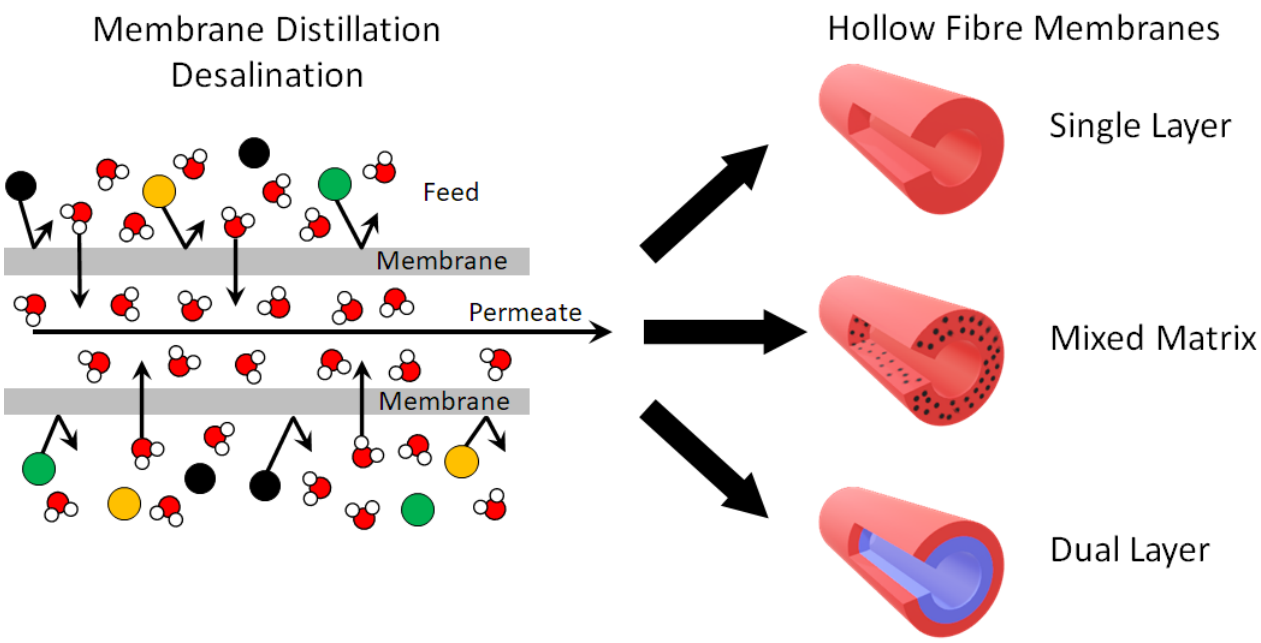

# Hollow fibre polymeric membranes for desalination by membrane distillation technology: A review of different morphological structures and key strategic improvements

Marcello Pagliero[1], Mohamed Khayet[2,3], Carmen García-Payo[2], Loreto García-Fernández[2]

[1] *Department of Chemistry and Industrial Chemistry, University of Genoa, Via Dodecaneso 31, 16146, Genoa, Italy*

[2] *Department of Structure of Matter, Thermal Physics and Electronics, Faculty of Physics, University Complutense of Madrid, Avda. Complutense s/n, 28040, Madrid, Spain*

[3] *Madrid Institute for Advanced Studies of Water (IMDEA Water Institute), Calle Punto Net Nº 4, 28805, Alcalá de Henares, Madrid, Spain.*

** Corresponding author: khayetm@fis.ucm.es*

*Tel. +34-91-3945185; Fax. +34-91-3945191*

## Abstract

Membrane distillation (MD) is a separation technology that is gaining increasing importance for desalination because of its optimal separation performance and its ability to treat highly concentrated saline solutions. Among all membrane morphological structures, hollow fibre (HF) exhibits some peculiar advantages, does not require any support to withstand the operation conditions and can be arranged in modules reaching high packing density and optimal fluid dynamics reducing both temperature and concentration polarization effects on MD desalination performance. In general, hollow fibre membranes are prepared by spinning a dope solution following different techniques. The HF membrane morphology can be tuned by modifying a large number of spinning conditions as well as by improving the membrane structure by preparing single layer, mixed matrix or dual layered hollow fibres. This review analyses the research studies developed so far on the design and preparation of different types of hollow fibres together with a critical evaluation of the effects of the involved preparation conditions on MD desalination performance, and some useful remarks to improve hollow fibre characteristics, desalination performance and thermal efficiency. Among the proposed HF for MD desalination, dual layered HF membranes exhibit high permeate fluxes up to 98.6 kg/m$^2$h with good salt rejection factors.

**Keywords:** Hollow fibre; Membrane distillation; Desalination; Single layer; Mixed matrix; Dual layer; Thermal efficiency.

**Highlights:**

Review on single layer, dual layer and mixed matrix hollow fibres prepared by NIPS & TIPS techniques
Hollow fibre membranes are engineered for desalination by membrane distillation (MD)
The coagulant strength and the use of additives improve the MD membrane performance
Creation of aggregates limits the development of mixed matrix hollow fibre membranes
Delamination is a major problem in the production of dual layer hollow fibres

**Graphical abstract**

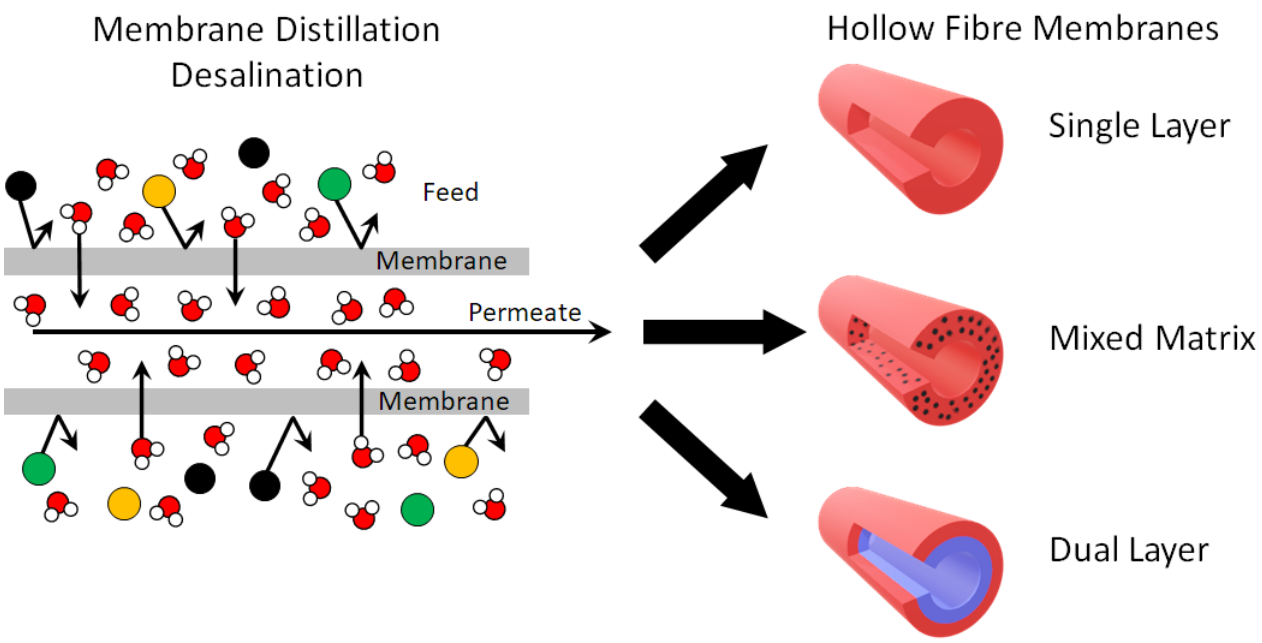

# 1. Introduction

Water scarcity has become a growing problem that needs to be addressed with improved and advanced technologies. Considering the available water resources, desalination technologies seem to be the easiest way to produce drinkable water. The idea of using membranes for water reclamation and sea water desalination was developed by the end of 1940s and the beginning of 1950s when the USA government started different research projects in order to face the water scarcity in California created by the increase of population [1]. The most renowned result of these projects was the preparation of the first reverse osmosis (RO) asymmetric membrane by Loeb and Sourirajan [2]. The subsequent rapid development of the RO process led to a decrease of the energy consumption of RO plants by almost 90% between 1970 and 2010 [3]. Because of its good energy efficiency, RO covered more than 65% of drinkable water production by worldwide desalination [4]. However, some issues such as the management of brines and discarded membrane modules should have been addressed [5].

One of the developed desalination technologies of emerging interests is membrane distillation (MD). It is a thermally driven separation process that uses a porous and hydrophobic membrane to allow the transport of water vapour and retain non-volatile compounds [6]. The MD driving force is the transmembrane vapour pressure difference driven by the transmembrane water chemical potential. Four main different ways can be followed to apply this driving force, namely direct contact membrane distillation (DCMD), air gap membrane distillation (AGMD), sweeping gas membrane distillation (SGMD) and vacuum membrane distillation (VMD) [6,7]. Other two hybrid MD configurations that have also been considered are liquid or material gap membrane distillation (LGMD or MGMD, respectively), which is a combination of DCMD and AGMD, and thermostatic sweeping gap membrane distillation (TSGMD), which is a combination of SGMD and AGMD. Compared to both pressure-driven membrane processes and traditional thermal processes, it was confirmed that MD exhibits various advantages. Regarding conventional distillation processes, MD allows the increase of the specific evaporation area by using an adequate membrane with a high porosity and a high membrane packing density, increasing this way the water production rate and reducing the necessary surface of the desalination system. Moreover, by operating at low temperatures, it is possible to exploit low grade thermal sources such as solar, industrial heat waste streams and geothermal sources [5]. Compared to RO, the pressure involved in MD technology is by far much lower. Therefore, lower mechanical strength is required for MD membranes, which should have the necessary mechanical properties to be assembled in modules and withstand the hydrostatic pressure generated by the circulating fluids through the feed and permeate channels. In contrast to RO, MD can reach very high rejection of non-volatile solutes, greater than 99.9% [8], and the feed concentration has minor effects on both water permeate flux and salts rejection factor. Consequently, MD can be integrated with crystallisation process to achieve zero liquid discharge to the environment resolving this way the brine management problem of RO plants [9,10].

One of the key factors that must be improved in order to increase MD performance is the membrane itself. In fact, the majority of the membranes currently used in MD pilot plants are initially intended for other purposes (e.g. microfiltration) rather than MD applications. Therefore, the development of proper and specific MD membranes with improved water production rate and specific energy efficiency is a key element towards the industrial implementation of MD technology [11]. Generally, MD membranes should be highly porous in order to reduce both the mass transfer resistance and the thermal conductivity and provide a high permeance together with a high thermal efficiency. Meanwhile, the membrane should not be wetted by the process liquid to avoid feed leakage and permeate contamination [8]. For this reason, MD membranes are usually prepared using hydrophobic polymers like polytetrafluoroethylene (PTFE), polypropylene (PP) or polyvinylidene fluoride (PVDF ) among other polymers and copolymers [12].

There are different MD membrane morphological structures such as, flat sheet, tubular and hollow fibre (HF), and nanofibrous membranes. The most used are the flat sheet ones that can be arranged in both plate and frame and spiral wound modules in order to obtain a good packing density. The plate and frame modules can be used with high specific flow rates to decrease the boundary layer adjoining the membrane surface promoting this way a high turbulence, low polarisation effects and reduced fouling phenomena. However, this structure is limited by a poor packing density with a typical specific surface area between 100 and 400 $m^2/m^3$. On the contrary, spiral wound membrane modules are widely used in RO process because of their higher packing density (300-1000 $m^2/m^3$). However, these modules need proper feed spacers in order to promote turbulence within the feed channels without causing significant pressure drops [13,14].

It is worth quoting that hollow fibre modules can reach a packing density up to 9000 $m^2/m^3$ by arranging in modules either straight fibres without the use of any support, twisted or curled fibres and knitted fibres in spacers to improve the fluid dynamics and promote the necessary turbulence to reduce polarization and fouling effects [15,16]. These features made the interest in hollow fibre membrane grow during last years as can be seen in Figure 1 that reports the number of papers published each year between 1992 and December of 2020 on hollow fibre application in MD process.

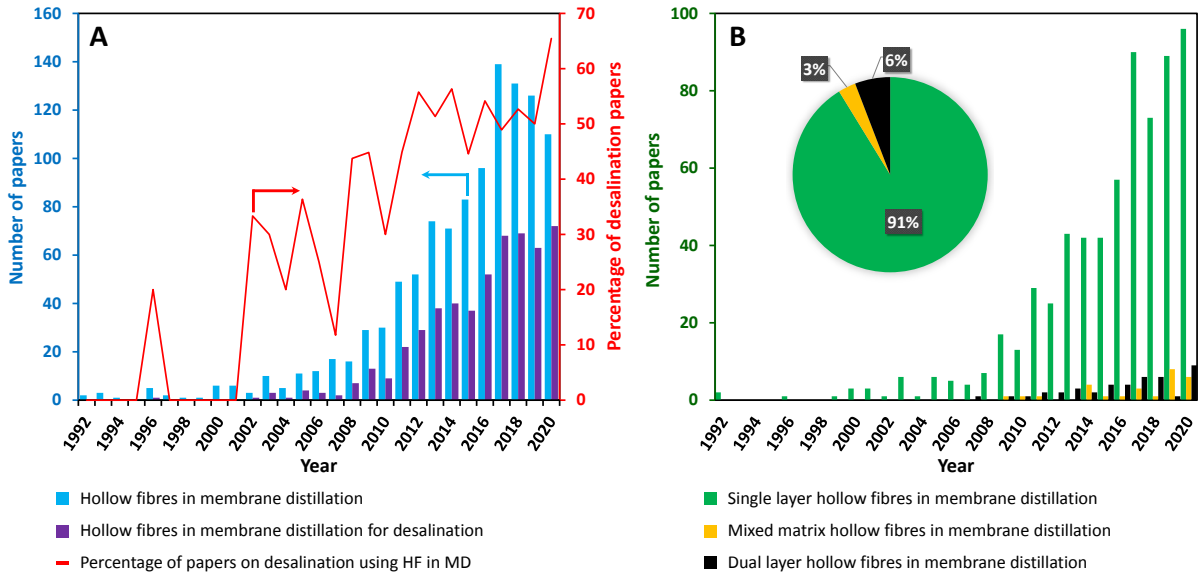


*Figure 1. (A) Number of papers published in international refereed journals each year since 1992 on hollow fibre membranes for MD (blue) and those papers focused on MD desalination using hollow fibre membranes (purple). The red curve shows the percentage of papers devoted to desalination among those published papers on MD using hollow fibre membranes. (B) Number of papers published about single layer (green), mixed matrix (yellow) and dual layer (black) hollow fibres used in MD.*

This review is devoted to the analysis of hollow fibre membrane preparation for MD technology with special application in desalination. The effects of the preparation parameters on the morphological structure of different types of hollow fibres prepared with different techniques together with their MD desalination performance are outlined. Three different hollow fibre morphological structures are addressed, single layer, mixed matrix and dual layer hollow fibres. Critical remarks are outlined in order to improve hollow fibre characteristics and desalination performance and efficiency. The description of MD application in large scale, the effect of the membrane module design and the study of HF fouling/scaling phenomena can be found in some other interesting review manuscripts [15,17–19].

## 2. Hollow fibre membrane preparation techniques

The main processes used to prepare HF are the nonsolvent induced phase separation (NIPS) and the thermally induced phase separation (TIPS). The effects of the different NIPS and TIPS parameters on the hollow fibre structural morphology and MD desalination will be explained in the following sections.

In NIPS, the solvent is removed from the solution by extracting it using a nonsolvent, which is a substance that is miscible with the solvent, but it is unable to solubilize the polymer. Removing the solvent from the solution increases the polymer concentration up to its solubility limit causing its precipitation [20]. The membrane structure can be tuned by modifying preparation parameters, such as the polymer concentration, the strength of the nonsolvent system [21], and by using additives as discussed later on.

In the TIPS technique, the phase separation is achieved by decreasing the temperature of the dope solution. The polymer is dissolved in one or more solvents – usually called diluents – at a high temperature in order to obtain a homogeneous solution. The dope solution is then extruded through a spinneret at high temperature and immersed in a low temperature quenching bath where it is cooled. At low temperature the diluents are not able to solubilize the polymer and the solution undergoes a phase separation [22]. Once the hollow fibre membrane is formed, the remaining solvent is removed using cleaning baths [23]. Both the properties of the diluent and the solution viscosity play a major role in defining the final membrane morphology. Moreover, differently from NIPS, TIPS is a non-isothermal process and the cooling rate of both the internal and external side of the HF can greatly modify the solidification process and the HF structure. For more specific details, NIPS and TIPS are treated extensively in other publications [24,25].

# 3. Single layer hollow fibre membranes

Single layer hollow fibre (SLHF) membranes are prepared by extruding a homogeneous dope solution through a spinneret. During the preparation of HF, following either NIPS or TIPS technique, the most important part of the whole spinning setup is the hollow fibre spinneret, since it imposes the main geometrical characteristics of the nascent hollow fibre membrane [25].

## *3.1. Spinneret design*

Generally, the spinneret is constituted by a reservoir and an annular channel designed to improve the polymer solution distribution and obtain an uniform flow [26]. Several works looked at the effects of the spinneret on the morphology and performance of the hollow fibre while others proposed new designs to optimise the flow patterns inside the HF.

When a viscous polymer solution is forced to circulate through a thin channel, shear forces induce some molecular orientation that affects the membrane morphology and performance [27]. Changing the spinneret channel design can modify the stress applied and the grade of chain orientation. Wang et al. [26] compared a traditional straight channel spinneret with one characterised by conical channels (Figure 2) and found that, using the conical spinneret, macrovoids were always present in the membrane cross section at every tested extrusion flow rate; but when the straight channel spinneret was used at high flow rate, the macrovoids were suppressed.

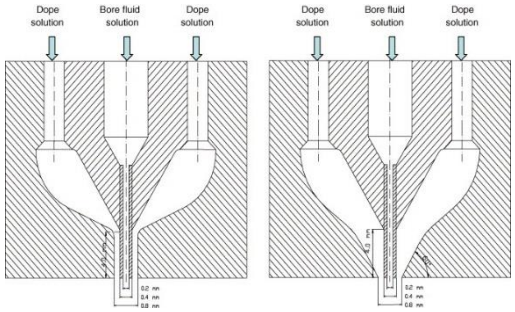


*Figure 2: Schematic diagrams of dual-orifice spinnerets with different flow angles (90° and 60°). Adapted from* [26].

The spinneret channel geometry has also been tuned in order to impose some peculiar shapes to the HF in order to increase the membrane surface area per volume and improve the fluid dynamics in the feed channel of the membrane. Microstructured channels were designed [28–31] to prepare HF membranes with corrugations at the inner or outer surfaces. In particular, García-Fernández et al. [30] applied this approach to prepare HF made of poly(vinylidene fluoride-*co*-hexafuropropylene), PVDF-HFP, for MD applications. They designed a triple-orifice spinneret illustrated in Figure 3A. By changing the piece (P) of this spinneret, it was possible to prepare both traditional circular HF and star shaped HF shown in Figure 3B. Moreover, with this type of spinneret an external coagulant can be circulated through its outermost channel in order to reduce or remove the commonly formed skin layer at the outer surface of the HF and to retain the transfer microstructure shape on the outer surface.

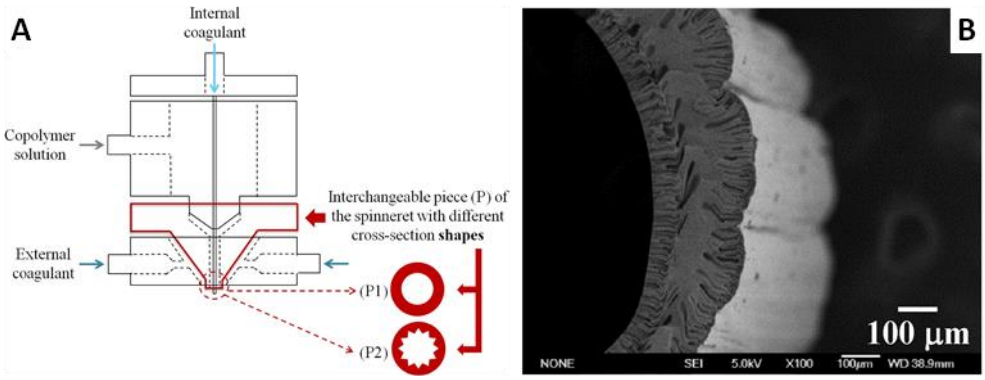


*Figure 3: (A) Scheme of the triple-orifice spinneret and (B) corrugated membrane. Adapted from* [30].

It was claimed that the corrugations enhanced the external effective surface area of the fibres available for water vapour condensation and act as micro-turbulence promoters mitigating the temperature polarization effect and improving the MD mass transport as consequence. However, large corrugations did not always induce an improvement of the MD permeate flux [30].

A different approach to increase the turbulence inside the HF lumen was considered by Luelf et al. [32] exploiting the concept of static mixers used in plug flow reactors. To implement this geometry in the HF, it was necessary to develop a rotating system that allowed also the feeding of both the bore fluid and the polymer solution (Figure 4A). The bore fluid is fed through the inner capillary of the assembly while the

polymer solution is fed from the side opening in a wider tube that allows the use of high viscosity polymer solutions. The polymer solution inlet stands still while the tubing above and below the adjacent rotary couplings are rotating. Therefore, the inner capillary is rotating together with the spinneret inside the still-standing polymer inlet t-piece.

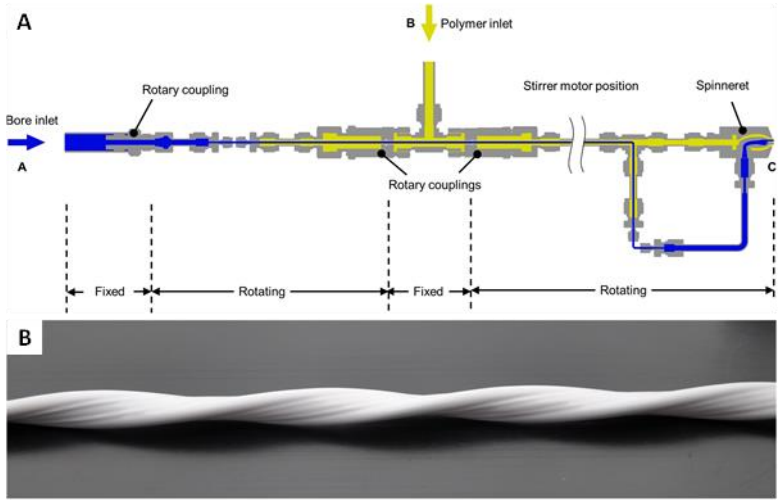


*Figure 4: (A) Scheme of the rotating spinneret system and (B) image of the prepared membrane. Adapted from* [32].

Fluid dynamics improvement by exploring a new spinning design was also addressed by Luelf et al. [33] and Roth et al. [34], who prepared HF with a sinusoidal inner shape. The bore fluid line contained a pulsation device that applied a variable bore fluid flow inside the nascent fibre (Figure 5A). The increase of the bore fluid flow created a periodic variation of the HF diameters (i.e. formation of waves) as showed in Figure 5B.

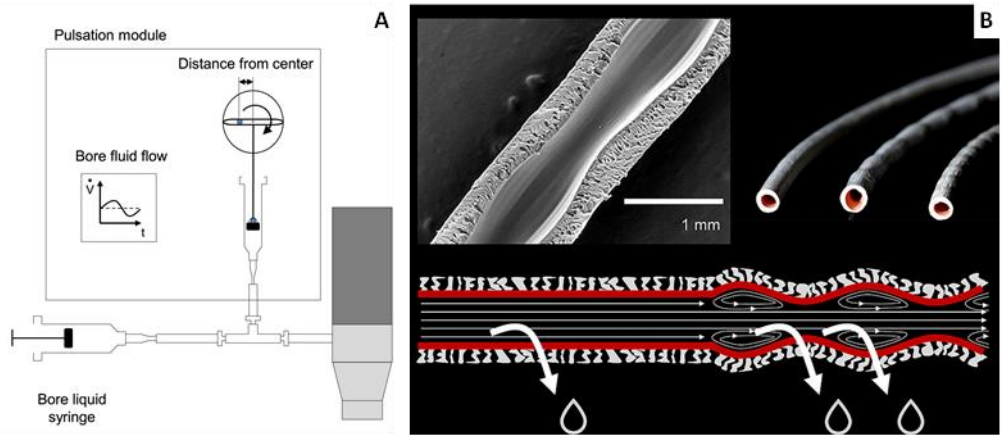


*Figure 5: (A) Pulsating device connected to bore fluid flow tubing creates sinusoidal variation in bore fluid flow; (B) Image and scheme of the prepared HF. Adapted from* [34].

### *3.2. Spinning conditions*

Depending on the HF formation technique, different spinning conditions can be modified to obtain the desired HF membrane morphology and performance. For NIPS, the main parameters that must be tuned are the interactions between the polymer and the nonsolvent. In order to obtain specific morphologies, it is common to use different nonsolvents as bore fluid and external coagulant. This is a key factor determining

the membrane cross section structure as well as its hydrophobicity and porosity. Instead, for TIPS the diluent-polymer interactions become of major impact. Besides, the polymer concentration as well as the bore fluid and quenching bath temperatures can have great influence on the phase separation mechanism, leading to different morphological structures.

### *3.2.1. Gap type and gap distance*

The air gap (AG), which is the distance between the tip of the spinneret and the top surface of the external coagulation bath, has multiple influences on the final membrane structure. When the extruded polymer solution travels through air gap distance before being immersed in the coagulating bath, it is called dry-wet spinning; when the AG distance is set to zero, the spinning technique is defined as wet spinning; and when the outer surface of the nascent HF is wet along the gap distance, it is called wet/wet spinning. At the exit of the spinneret, the polymer solution is affected by the die swell due to its viscoelastic and surface tension properties while coagulation starts at the inner surface of the as-spun hollow fibre for the dry/wet spinning technique, and at both the inner and outer surfaces for the wet or wet/wet spinning technique. For the wet/wet spinning technique, the wetting mode of the outer layer can be performed using a double spinneret (i.e. triple-orifice spinneret), the external coagulant circulates through its outermost channel, wetting longitudinally the nascent HF along the gap distance [35]; or by using a simple spinneret and spraying the coagulant towards the outer layer of the nascent HF placing various micro-jets along the gap distance [30]. This latter novel methodology was used to successfully induce corrugations on the outer surface of the hollow fibre because the coagulant pressed inwards the wall of the nascent membrane.

Throughout the air gap length, the dope solution is affected by different phenomena, such as solvent evaporation, molecular chain orientation and gravity induced elongation [36]. At high AG distance, the weight of the nascent fibre elongates the dope solution creating fibres with smaller diameters and wall thickness. In some cases this effect can result in rupture of the nascent fibre or in its collapse [25]. In general, as the AG is increased, the nascent fibre takes longer times to reach the external bath. Therefore, a larger amount of solvent can evaporate from the external layer increasing the polymer concentration on the external surface, inducing the formation of the undesirable dense skin-layer. When semi crystalline polymers are used, the solvent evaporation also leads to an increase of both spherulites dimension in the outer layer and porosity [36]. Tang et al. [37] registered a turning point of the overall porosity at 9 cm air gap length (i.e. the overall porosity was increased until an air gap length of 9 cm and further increases of the AG resulted in a decrease of both the overall porosity and the MD permeate flux). Khayet et al. [38] and Wang et al. [39] observed a decrease of the porosity and the pore size as the AG was increased. This phenomenon was related to the greater molecular orientation and compact polymer chain.

Attempts have been made changing the gas in the gap space between the spinneret and the external coagulation container. Khayet et al. [40,41] prepared polyethersulfone (PES) ultrafiltration HF via NIPS using

five different gases (air, oxygen, nitrogen, carbon dioxide and argon) through the gap distance of 28 cm of the spinning system. Maintaining the same all spinning conditions, it was claimed that the gas induced morphological changes at the outer surface of the HF. In particular, pore size, surface roughness and nodule size of the external layer of the HF were influenced by the type of the gas while the internal surface was not modified. To the best of our knowledge, this effect has not been studied yet for the preparation of hydrophobic HF membranes for MD application.

The air gap effect becomes more important in TIPS technique because of the higher temperature of the dope solution compared to NIPS technique. When volatile diluents are used, the evaporation can greatly increase the polymer concentration at the outer layer resulting in an almost dense, poorly permeable outer skin [42,43]. However, this effect can be neglected when non-volatile diluents are used [36]. When the diluent evaporation is slow, the air gap mainly affects the spherulites growth. For a short air gap distance, the polymer solution reaches the quenching bath faster and the spherulites do not have enough time to grow resulting in a lower porosity of the outer surface. With the increase of the air gap, bigger spherulites are produced and the HF membranes present improved permeability [36,44].

### *3.2.2. Effect of spinning solution composition*

One of the major parameters that can be tuned to obtain the needed characteristics of the HF is the polymer solution composition. By selecting proper polymer solution materials, it is possible to modify the solution properties (i.e. viscosity and surface tension) in different ways, such as the polymer molecular weight and its concentration [37,45,46], type of additives for pore formation and its concentration, nanoparticles, solvent(s)/diluent(s), etc. [47–49].

One intrinsic characteristic is the viscosity of the spinning polymer solution. In general, in order to obtain a HF with proper mechanical strength and pore size, a critical value of the viscosity is required. The solution viscosity greatly affects the coagulation path followed by the polymer, both in NIPS and TIPS techniques, regulating the solvent-nonsolvent exchange rate. The easiest way to increase the dope solution viscosity is to increase the polymer concentration or the polymer molecular weight. The increase of the polymer concentration in the spinning solution leads to an increase of the HF wall thickness and a decrease of the overall porosity of the membrane, reducing the MD permeate flux as a consequence [37,45,46]. Nevertheless, it was also stated that the increase of the polymer concentration, increases the viscosity and reduced therefore the die swell at the exit of the spinneret, and the subsequent external diameter together with the thickness of the HF [50]. In fact, the surface tension also affects die swell and the dimensions of the HF.

Tang et al. [37] verified the effect of PVDF concentration on the morphology and performance of membranes prepared via NIPS. By increasing the polymer concentration from 13 to 17 wt%, it was registered an enhancement of the density and thickness of the inner and outer surface layers together with a reduction

of the macrovoids size. With the lowest concentration, finger-like voids were formed under both the inner and outer layers and reached the centre of the HF wall. This induced the highest overall porosity (79.2%) and resulted in the highest DCMD permeate flux when using 9% NaCl aqueous solution (almost 16 kg/m$^2$h with $T_f$ = 65°C, $T_p$ =20°C). By increasing the polymer concentration from 13% to 17% led to a decrease of both the porosity (75.0% and 69.6%, respectively) and the permeate flux (almost 14 and 10 kg/m$^2$h, respectively). The same results were confirmed by García-Payo et al. [51] for PVDF-HFP copolymer. The membrane cross section shifted from a finger-type structure when the lowest copolymer concentration (17 wt%) was used, to a sponge-type structure through the whole cross section of the HF membrane prepared with the highest copolymer concentration (24 wt%). This change of the membrane morphology reduced the pore size, the porosity and the DCMD performance. For semi crystalline polymers, like PVDF, a great change of the membrane morphology occurs when the coagulation rate is modified. In fact, limiting the solvent-nonsolvent exchange, the coagulation path becomes dominated by the so called solid-liquid demixing that creates a globular interconnected structure [52]. Wang et al. [53] added a weak nonsolvent (e.g. ethylene glycol, EG) in the spinning PVDF/NMP (N-Methyl-2-pyrrolidone) solution in order to modify the coagulation path and the membrane structure. By adding EG to the spinning solution, the porosity was increased from 68.5% to 73.8% and the permeate flux was enhanced from almost 9 kg/m$^2$h to 41.5 kg/m$^2$h (for DCMD of 3.5% NaCl aqueous solution at $T_f$ = 80°C and $T_p$ = 20°C).

Yao et al. [54] evaluated the effect of different nonsolvents additives (e.g. acetone, dibutyl phthalate, DBP; and toluene) on the membrane morphology. The interplay between the dope solution parameters generated HF with significantly different structures and DCMD performance. The dope solution viscosity and its water affinity governed the phase separation process favouring L-L or S-L demixing. The first mechanism was more dominant when the dope solution had lower viscosity and higher water affinity (e.g. acetone) generating membranes with lower porosity and pore size together with as worse DCMD performance. In contrast, S-L demixing was the main mechanism when nonsolvents with lower water affinity and higher viscosity were added to the dope solution (e.g. DBP). The formed membranes in this last case exhibited larger pores suffering the risk of their wetting in MD tests. By adding to the polymer solution, a nonsolvent with low viscosity and low water affinity such as toluene, resulted in membranes with a symmetric structure composed by small spherulites. This morphology induced a large porosity and a small pore size, ensuing good and stable DCMD permeate fluxes (18.9 L/m$^2$h, 7 wt% NaCl solution at $T_f$ = 60°C and $T_p$ = 20°C).

Wu et al. [55] investigated the effect of the PVDF-HFP concentration in the PVDF dope solution on the morphological structure and DCMD performance of SLHF membranes. The objective of the research study was the increase of the hydrophobic character of the HF by increasing the fluorine content of the polymeric material. The addition of the copolymer, as well as the increase of its concentration from 1.5 to 4.5 wt%, improved the water contact angle from 79° to 96°. However, the overall porosity of the HF was reduced and thus the DCMD permeate flux was decreased from 11.9 kg/m$^2$h (5 wt% NaCl solution, $T_f$ = 60°C, $T_p$ = 17°C)

when the PVDF dope solution was used without PVDF-HFP, to 6.0 kg/m$^2$h when the highest PVDF-HFP concentration was used.

When the HF membranes were prepared by TIPS technique, the increase of the dope viscosity hinders the mobility of both the polymeric chains and the diluent molecules. The accumulation of polymer molecules can favour the crystallisation process [56] and a reduction of the membrane porosity and pore size [44]. Karkhanechi et al. [45] investigated the effect of the polymer concentration using ethylene chlorotrifluoroethylene copolymer (ECTFE) and two diluents (diethyl phthalate, DEP and glycerol triacetate, GTA). In their work, they highlighted a sudden decrease of water permeability when the concentration was increased from 20 to 30 wt% while the mechanical properties of the membranes was increased, independently from the diluent used. Zhou et al. [57] tested the same polymer obtaining similar results. Moreover, they found a modification in the solidification path based on the polymer concentration, as reported in Figure 6. When the ECTFE concentration ranged from 10 to 50 wt% (Figure 6 A-E), liquid-liquid phase separation with subsequent polymer crystallization occurred, while solid liquid phase separation became the only path for polymer coagulation when its concentration was 60 wt% (Figure 6 F). Moreover, the authors claimed that in the two extreme cases (10 and 60 wt%) the two solutions resided in the metastable region and the phase separation proceeded via nucleation and growth. However, the other compositions led to spinodal decomposition phase separation.

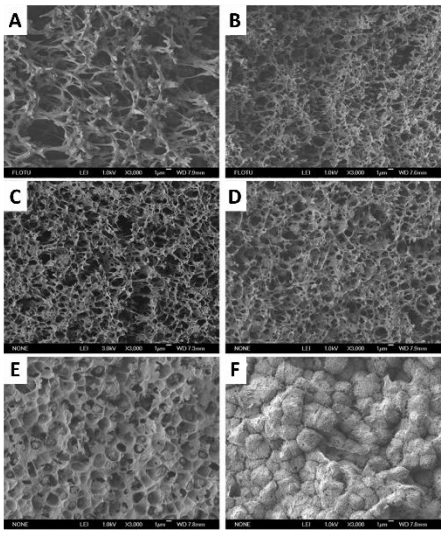


*Figure 6: Cross section morphologies of ECTFE membranes prepared from ECTFE–binary diluent systems with various ECTFE concentrations: (a) 10 wt%, (b) 20 wt%, (c) 30 wt.%, (d) 40 wt%, (e) 50 wt%, and (f) 60 wt%. Adapted from* [57].

Hassankiadeh et al. [44] prepared HF membranes using different molecular weight PVDF. By decreasing the polymer molecular weight, the solution viscosity was reduced and the polymer chain orientation was enhanced resulting in lower surface roughness. However, the overall porosity and the mean pore size were increased. These differences in membrane morphology resulted in a change of the DCMD performance of the membranes. Using a polymer with lower molecular weight resulted in higher permeate

fluxes. This finding is in contrast to what was claimed by Matsuyama et al. [43], who prepared HF using two different high-density polyethylene (HDPE). The membranes prepared with the lower molecular weight HDPE showed smaller pore size and lower water permeability. This was related to the higher mobility of the diluent molecules in low viscosity solutions that allowed a greater evaporation in the air gap and a greater increase of the polymer concentration on the outer surface of the HF.

Another parameter that can be explored to tune the HF morphology is the solvent used to prepare the polymeric solution by NIPS technique. García-Fernández et al. [58] used different mixed solvents (N,N-dimethylacetamide, DMAc; N,N-dimethylformamide, DMF; and trimethyl phosphate, TMP) to prepare PVDF-HFP hollow fibres. The change of the solvent medium affected considerably both the spinning solution viscosity and the solvent-copolymer-nonsolvent interactions. With the increase of the dope viscosity or the reduction of the interactions between the solvent and nonsolvent, the precipitation rate was reduced inhibiting the formation of macrovoids, which typically act as weak points reducing the mechanical properties and the resistance of the membrane to wettability. When TMP was added to the solvent medium, HFs with higher mean roughness of the external surface and greater mean pore sizes were obtained. The DCMD permeate flux was increased from 54 kg/m$^2$h to 68 kg/m$^2$h when the DMAc/TMP ratio was increased from 100/0 to 60/40 (Feed: NaCl 3 wt%; $T_f$ = 80°C; $T_p$ = 25°C).

The membrane properties can also be tuned by introducing different kind of additives into the spinning solution. For NIPS, one of the most investigated additives category are the so called pore forming agents that can be inorganic salts (e.g. LiCl, $BaCl_2$) [37,59] or low molecular weight polymers that can be dissolved in water like polyethylene glycol (PEG) [20,37,60] and polyvinyl pyrrolidone (PVP) [59,61]). The use of pore forming agents allows the improvement of the membrane porosity and effective active surface for vapour transport, increasing therefore the MD permeate flux.

Kong and Li [59] verified that adding LiCl and PVP to the PVDF solution resulted in higher porosity membranes but with reduced hydrophobic character. These results were confirmed by Tang et al. [37], who reported that an increase of the LiCl concentration in the spinning solution resulted in a more porous sponge-like structure. Moreover, they investigated the effect of PEG-400 as oligomeric pore forming agent. The great affinity of PEG with water induced fast phase separation and favoured the formation of macrovoids. These effects led to an enhancement of the DCMD permeate flux from 1 up to 9 kg/m$^2$h ($C_f$ = 9% NaCl, $T_f$ = 65°C, $T_p$ = 20°C).

Similar results were obtained by Li et al. [20], who confirmed the formation of big macrovoids and denser skin layer when PEG-400 was added to the spinning solution, and by Huo et al. [60], who also observed an increase of the porosity from 68.7% up to 79.7% and an enhancement of the water contact angle from 86° to 105° by adding both LiCl and PEG-1500 to the PVDF spinning solution. The introduction of pore forming agents increased dramatically the DCMD performance from almost 10 kg/m$^2$h to 41 kg/m$^2$h when using 3.5% NaCl aqueous solution ($T_f$ = 80°C and $T_p$ = 20°C).

Simone et al. [61] investigated the effect of PVP as pore forming agent and found that the effect on the membrane structure highly depends on its concentration. At low concentrations (from 0 to 11 wt%), the addition of PVP favours the formation of macrovoids, increases the total porosity, but affects the mechanical properties of the membranes. Further addition of PVP (15 wt%) creates a sponge structure with a small decrease of porosity but with better mechanical strength. The change of the porosity was then confirmed by VMD tests observing and increase of the permeate flux from 4.3 kg/m$^2$h when no PVP was used, to 17.9 kg/m$^2$h when 9% of PVP was added, whereas further increase of PVP up to 15 wt% resulted in a permeate flux decline to 15.3 kg/m$^2$h.

Another way to modify the dope solution is the addition of nanoparticles that can improve membrane mechanical properties, hydrophobicity and MD performance as will be described in the next section.

A parameter that plays a major role on the final membrane morphology is the selection of the diluent when applying TIPS technique. The interactions between polymer and diluent affect the thermodynamic properties of the solution as schematized in Figure 7.

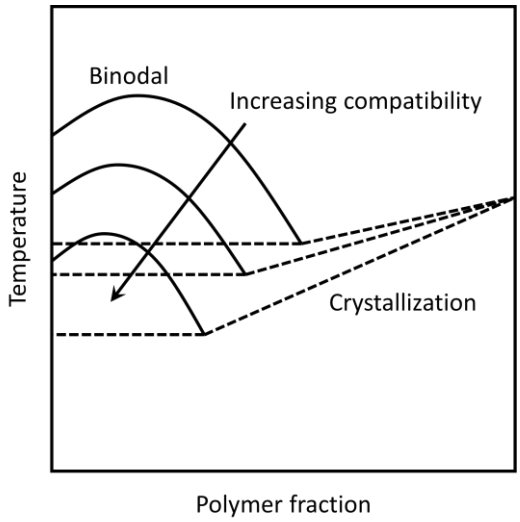


*Figure 7: Schematic phase diagram in TIPS process.*

When the compatibility of the two components is weak, the binodal line is moved towards higher temperatures while the crystallization line is less influenced. The polymer solidification proceeds via liquid-liquid phase separation followed by crystallization [62,63], and results in longer time for pore growth during the cooling step [64]. However, when the interactions between diluent and polymer are strong, the binodal curve is moved towards lower temperatures and the system first undergoes solid–liquid phase separation via nucleation and growth path [65]. To prepare membranes with specific properties, the interactions between the polymer and the diluent system can be tuned using a mixture of diluents with different compatibilities [56,57,65–67]. Gu et al. [66] investigated the effect of different diluent mixtures on PVDF membrane morphology. As the interactions between the polymer and the diluent mixture decreased, the spherulitic structure became less evident and the porosity increased. Song et al. [65] prepared two sets of

HF comparing the morphologies and MD performance of membranes prepared by systems with lower and higher compatibility. The interactions between polymer and diluent were tuned by increasing the concentration of a weak diluent dioctyl phthalate (DOP) in γ-Butyrolactone (γ-BL) from 53.5 to 58.4 v/v%, obtaining the structures reported in Figure 8A and B respectively.

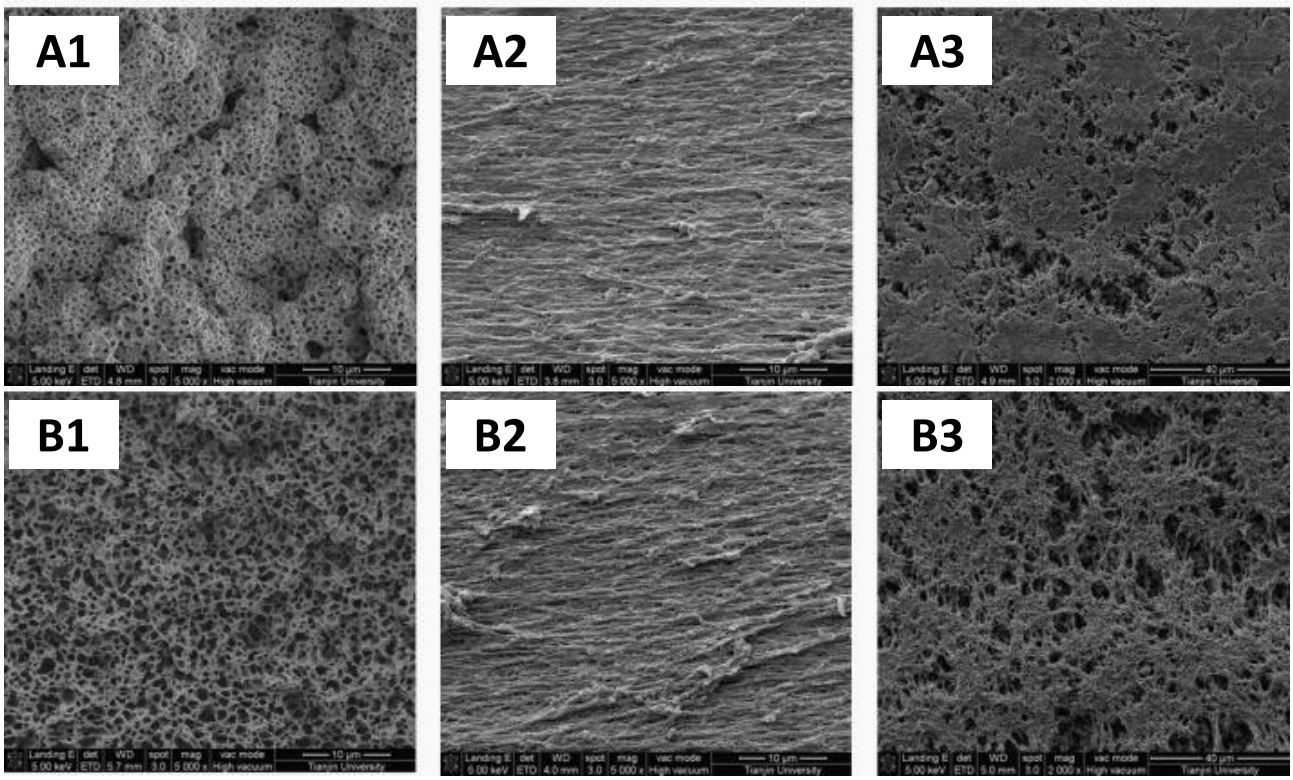


*Figure 8: SEM morphology of the PVDF hollow fibre membranes prepared from the system A: PVDF 12.81 wt%, DOP 53.50 v/v% and B: PVDF 12.74 wt%, DOP 58.44 v%. (1) middle structure, (2) outer surface and (3) inner surface. Adapted from* [65].

The system A was characterised by stronger interactions between the polymer and the diluent mixture. The final structure was influenced by the competition between the two kinds of phase separation mechanisms and the final morphology was characterised by spheres, created by the Solid–Liquid phase separation, with an open cell morphology generated by the Liquid–Liquid phase separation. Decreasing the interactions between the polymer and the diluent mixture (system B), the gap between binodal curve and crystallization curve became larger and the membrane morphologies were totally dominated by cellular structures, which resulted from pure Liquid–Liquid phase separation. The membrane prepared using mixed diluents with weaker interactions exhibited a slightly large mean pore size and porosity and improved the DCMD permeate flux that increases from 20.8 kg/m$^2$h (for the system with strong interactions, A) up to 51.5 kg/m$^2$h (for the system with weaker interactions, B) when treating a 3.5% NaCl aqueous solution at 90°C ($T_p$ = 20°C).

### *3.2.3. Bore fluid or internal coagulant*

The structure of the internal layer of hollow fibres can be tailored using a different bore fluid (BF) that permits to change its coagulation mechanism. Various research studies have been focused on the effect of bore fluid chemical composition, its temperature and flow rate. For NIPS technique (Figure 9), the choice of a strong BF, like water, results in a fast precipitation of the polymer that creates an almost dense superficial layer supported on a macrovoids layer. On the other hand, by using a weak internal coagulant, the precipitation rate is slowed and a rougher more porous structure is created [68,69].

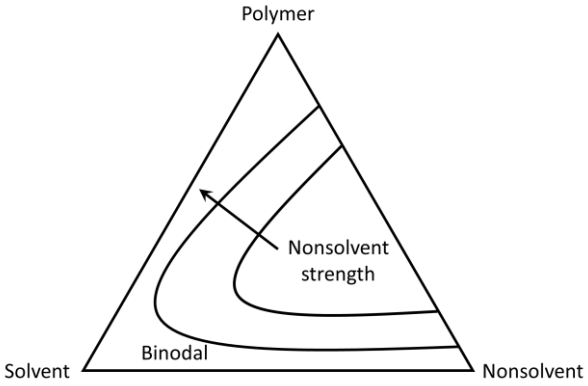


*Figure 9: Schematic phase diagram during NIPS process.*

The choice of the adequate BF composition can be done based on its solubility parameters compared to those of the spinning polymer solution. When the difference between solubility parameters is low, the BF acts as a weak nonsolvent, whereas it is a stronger nonsolvent for larger difference [70].In order to tune the nonsolvent strength two different ways have been considered: 1) adding additives like ethylene glycol (EG) [71], PEG [20] or PVP); 2) adding different amounts of the polymer solvent to water [70,72]. Li et al. [20] used water and PEG-200 as BF to prepare PVDF hollow fibres, and observed a great difference in their cross section morphology. In fact, using PEG-200 as BF, a membrane without finger-like macrovoids was prepared. The lower exchange rate between solvent and nonsolvent resulted in a lower precipitation rate that enhanced the formation of interconnected spherulites in the inner layer with an increase of the pore size and surface roughness as well as of the contact angle.

Garcia-Fernandez et al. [70] studied the effects of solvent (DMAc) in water mixture used as BF for the preparation of PVDF-HFP HF membranes. With the increase of DMAc concentration, it was possible to reduce the precipitation rate inducing a more open-porous inner layer with less macrovoids and creating an inner surface with larger pore sizes. The delayed phase separation also resulted in a narrower pore size distribution as well as a greater roughness. These morphology modifications led to an increase of the DCMD permeate flux from 6.8 kg/m$^2$h for water used as BF to 12.6 kg/m$^2$h for 60% DMAc/water solution as BF ($T_f$ = 80°C, $T_p$ = 25°C, NaCl 3% solution).

Fang et al. [73] investigated the effect of different BFs on the structure of PVDF HF membranes prepared by a triple orifice spinneret. The polymeric solution was extruded through the middle channel, while the pure diluent (propylene carbonate, PC) was circulated through the outermost channel of the spinneret in order to increase the external surface porosity of the HF. By analysing the compatibility of the BFs with both the diluent and PVDF in terms of Hansen solubility parameters, it was possible to control the inner layer structure and change the spherulites size and the pore dimensions. Using BFs with better compatibility with the diluent (PC) than with PVDF, reduced the polymer concentration at the membrane surface and induced the formation of isolated spherulites. The inner surface pore size became larger reaching values as high as 10 μm. On the contrary, BFs with a higher affinity with PVDF than with PC caused the opposite behaviour and the HF membranes showed smaller pores in the inner layer.

Other parameters of the BF that affect membrane formation are its temperature and flow rate. The main effect of flow rate variation is the modification of the HF thickness. By increasing the BF flow rate, its pressure swells the polymer film and increase the inner and the outer diameters, thinning the overall fibre thickness. Moreover, it also results in a faster precipitation of the polymer creating a macrovoid dominated structure with high porosity but low mechanical properties [74,75].

The BF temperature has great effects on the polymer coagulation path, affecting the solvent-nonsolvent interdiffusion. In addition, the viscosity of the inner layer of the dope solution is also affected. The polymer solution becomes less viscous with the increase of the BF temperature and the polymer chains have more time to move in organized structures. For semi-crystalline polymers, like PVDF, this results in a higher crystalline grade and spherulite dimensions in the HF structure [36]. Consequently, the porosity, mean pore size [36,37] and both the inner and outer diameters are increased [37].

The BF temperature is a major affecting parameter during membrane preparation by TIPS technique. In fact, it can change the solidification and crystallization path of the polymer solution. Increasing the bore fluid temperature, the inner layer and outer layers of the nascent HF are cooled at different rates. Therefore, the temperature decrease is slower in the inner layer than in the outer one and the spherulites are allowed to grow for longer times [44]. When both the quenching bath and the bore fluid were kept at ambient temperature, the HF exhibited a symmetric structure with small spherulites. Nevertheless, when the BF temperature was increased to 180°C, the inner layer underwent a slower cooling with respect to the outer layer. This resulted in bigger spherulites in the inner layer and smaller ones in the outer layer. This change of the inner layer morphology resulted in large pore size and high porosity.

### *3.2.4. External coagulant*

The external coagulant allows to complete the coagulation of the spun HF by inducing the polymer phase separation. However, its effects are different depending on the followed spinning method of

preparation. For NIPS, the external coagulation bath (ECB) is composed by a nonsolvent liquid that permits solvent removal from the dope solution and induces polymer solidification. For TIPS, the external bath is called quenching bath (QB) and its role is to lower the dope solution temperature below the solidification limit. In both cases, similarly to the BF, the external bath plays a major role on the morphological structure of the HF, in particular on its outer layer.

In NIPS technique, the strength of the coagulant exerts a great impact on the solidification rate of the membrane creating different structures. A strong nonsolvent in the ECB induces a fast precipitation of the polymer and the formation of a thin and almost dense skin layer with macrovoids beneath it, while a weak ECB produces a more symmetric, porous structure with a high surface roughness [76]. Several alcohols have been tested in order to change the strength of the nonsolvent, such as methanol [52], ethanol [52,77,78], isopropyl alcohol among others [52,79,80]. Particularly, Sukitpaneenit and Chung [52] compared the effects of increasing the amount of ethanol in the aqueous ECB (Figure 10) and the effects of using three different alcohols, methanol, ethanol and isopropanol (Figure 11), on the morphology of PVDF HF membranes prepared with the solvent NMP.

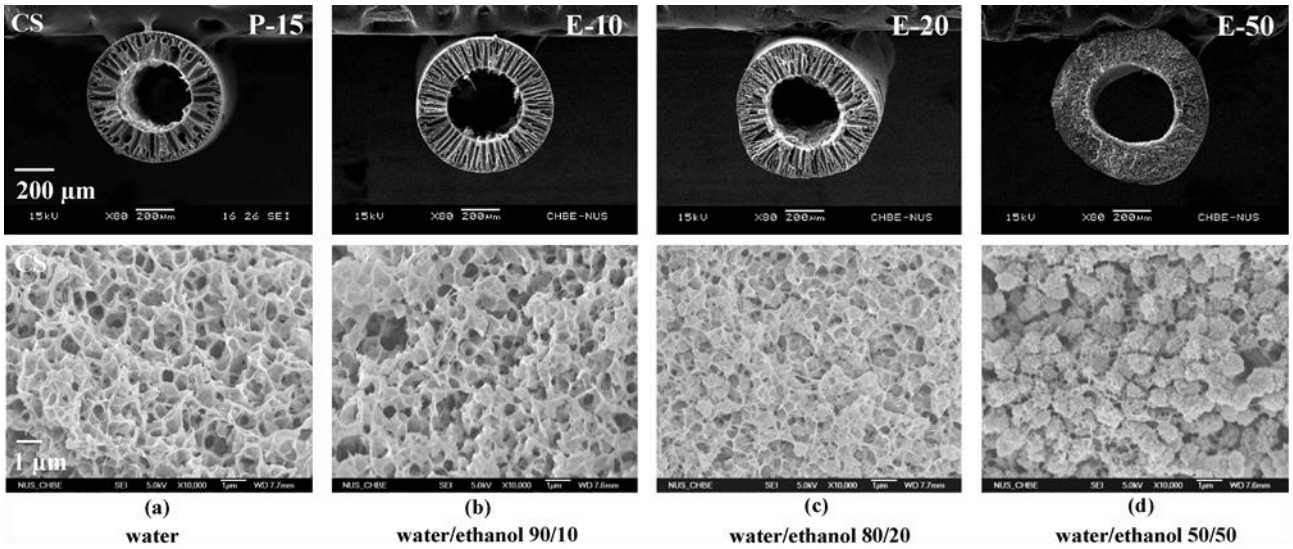


*Figure 10: Cross section morphology of HF membranes spun from 15 wt% PVDF/NMP with various compositions of water/ethanol external coagulation baths. Adapted from* [52].

By increasing the alcohol content in the ECB, the coagulation rate decreased and the finger-like macrovoids became first smaller and then eventually suppressed when the alcohol concentration reached 50%. In addition, the microstructure of the HF membrane switched from an interconnection of cavities to an interconnection of spherulites. Figure 11 reports the surface morphology of HF membranes prepared with different alcohols aqueous solutions as ECB. Under the same conditions, the change of the alcohol induced different spherulites packaging. As the affinity of the nonsolvent with the polymer was increased, the polymer crystallites needed more time to grow and a looser structure was formed.

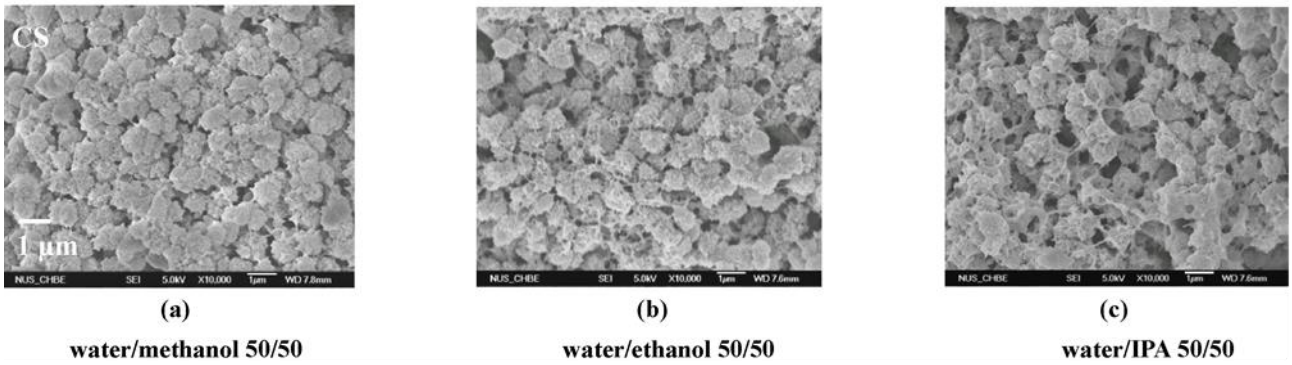


*Figure 11: Comparison of the cross-section morphology of PVDF hollow fibre membranes prepared with various water/alcohol mixtures as external coagulation baths. Adapted from* [52].

In other research studies, the harshness of the nonsolvent was tuned using solutions containing water and different amount of the polymer solvent [35,53]. García-Fernández et al. [35] investigated the effects of the external coagulant on the MD characteristics of PVDF-HFP hollow fibre membrane by increasing the solvent (DMAc) concentration from 0% (pure water) to 60%, when water was used as internal coagulant. For the highest DMAc concentration, the external layer of the HF cross section showed a denser structure with larger surface pores, while the inner layer remained characterised by large finger-like macrovoids. The same nonsolvent was also used as external and internal coagulant. By using DMAc/$H_2O$ 60% mixture, macrovoids free (fully sponge-like structure) HF could be prepared but its low thickness and mechanical properties hindered its MD desalination application. The reduction of DMAc content to 50% resulted in a stronger membrane with a DCMD permeate flux achieving 19.5 kg/$m^2$h for 3 wt% NaCl aqueous solution as feed. Apart from the strength of the nonsolvent, it is possible to tune the membrane outer layer morphology by changing the temperature of the ECB. In general, the solvent-nonsolvent exchange rate is increased at higher temperatures [81], resulting in a faster phase separation and the formation of a dense skin layer together with macrovoids [82].

For TIPS technique, the temperature of the quenching bath is the main parameter affecting the HF membrane structure. When the hot polymer solution gets into the QB, it suffers a rapid cooling. This rapid undercooling of the solution promotes the extensive formation of crystal nuclei [22].The high cooling rate hinders the nuclei growth and a large number of small spherulites is formed. Therefore, the HF membrane acquired an almost dense, low porosity structure, with a high tensile strength. When a higher temperature quenching bath is considered, the cooling rate is decreased and primary nuclei can grow for longer times, creating larger spherulites and inducing a more porous structure with lower tensile strength [43,44,66,83]. Ghasem et al. [83] confirmed the preparation of a more porous PVDF HF membrane with the increase of the quenching bath temperature. In addition, an increased pore size and crystallinity was observed, while the hydrophobic character was almost unchanged. Hassankiadeh et al. [44] obtained similar results for PVDF HF membranes, when investigating quenching bath temperatures between 3°C and 15°C. Since the crystalline

domains are known by their good thermal and chemical stability [84], the increase of the crystallinity degree of the membrane improved the chemical and thermal stability of HF membranes.

### *3.2.5. Spinning solution flow rate*

The spinning solution can be extruded from the spinneret by using a pump or applying a gas pressure on the dope solution container. In both cases the different extrusion flow rates influence the HF membrane morphology. Extensive and systematic researches have not been conducted for this spinning parameter but some comments can be pointed out on this regard.

Since polymer solutions are non-Newtonian fluids, when they are forced through the narrow gap of the spinneret, high shear stress are induced and different grades of chain orientation can be obtained causing a decrease of the membrane pore size [85]. This effect has a greater influence for a shorter air gap distance. In fact, by increasing the air gap length, the polymer chains of the external surface have more time to be rearranged before reaching the coagulation bath [86]. Moreover, at higher flow rates the polymeric chains of the inner layer are highly oriented and this structure is coagulated at the exit of the spinneret [87].

## *3.3. Thermal efficiency of single layer hollow fibre membranes*

MD thermal efficiency is influenced by the heat transfer by conduction through the membrane matrix. Generally, in MD three contributions to heat transfer occur simultaneously, the heat transfer associated to mass transfer (i.e. latent heat associated to both evaporation and condensation); the heat transfer by conduction through the void volume fraction (i.e. pores) of the membrane filled with gases and vapour, and the heat transfer by conduction through the membrane matrix. In this case, the thermal efficiency is defined as the ratio between the heat associated to mass transfer and the total heat transferred through the membrane [88]. In order to optimize the thermal efficiency of the MD process, the heat transfer by conduction through the membrane matrix must be reduced as much as possible maintaining a high permeate flux [89]. The best way is to increase the void volume fraction of the membrane and use materials with low thermal conductivity coefficients including mixed matrix membranes with low thermal conductivity coefficients.

In general, the thermal efficiency of MD process is enhanced when the feed temperature and/or the fluids flow rate in contact with the membrane surface are raised. In fact, the permeate flux increases exponentially with the feed temperature and the heat transfer by conduction through the membrane, considered heat loss in MD, is governed by the transmembrane temperature difference following Fourier' s law [25]. Increasing the fluids flow rate reduces the thickness of the boundary layer adjoining the feed and/or permeate sides of the membrane [30].

### *3.4. Remarks and future directions on single layer hollow fibre membranes*

Table 1 summarizes the characteristics and the MD performance of the HF prepared by different techniques under different conditions. The choice of important spinning parameters, in particular the dope solution composition together with both the internal and external coagulants are outlined, because of their significant effect on the membrane morphology (thickness, mean pore size, and porosity) as stated by various authors. For a correct data interpretation, the MD configuration and the operating conditions are also reported. Some data that were not directly available in the published papers have been extrapolated from the graphs using Quintessa© Graph Grabber 2.2 software. From the summarised data and other data available in the literature, some remarks can be drawn.

The addition of pore forming agents into the spinning solution has great effects on the membrane performance [37,61]]. In general, increasing their concentration results in a more porous structure and greater MD permeate flux. On the other hand, an excessive amount of additives can reduce the liquid entry pressure (*LEP*) of the HF membrane compromising therefore its salt rejection factor (i.e. permeate water quality). Therefore, a deep and systematic study on the effect of additives on the HF membrane structure must always be performed.

An alternative way to modify the membrane structure is by changing the coagulant strength [35,53,70]. By decreasing the polymer precipitation rate, it is possible to enhance the membrane porosity and the MD permeate flux as consequence. However, in the case of semi-crystalline polymers, the reduction of the coagulation rate can lead to the formation of spherulites with low interconnections, creating membranes with poor mechanical properties.

The majority of the published papers on the preparation of hollow fibres for MD is focused on the NIPS technique. The evaluation of TIPS, and mixed TIPS and NIPS techniques have been considered only by few membranologists [90,91] and the effects of the different involved parameters that control these processes must be investigated further. Compared to flat-sheet membranes, only two techniques, NIPS and TIPS, have been applied for the preparation of HF membranes for MD. Other techniques for HF engineering should be explored in order to tailor advanced single layer HF membranes for desalination by MD technology.

*Table 1: Preparation conditions and performance of single layer hollow fibres for MD.*

| Ref. | Technique | Dope solution composition (wt%) | BF | ECB | Thickness (μm) | Pore size (μm) | Porosity (%) | MD conditions | Permeate flux (kg/m²h) |
|---|---|---|---|---|---|---|---|---|---|
| García-Fernández et al. [35] | NIPS | PVDF-HFP/DMAc/TMP/PEG (19/30.4/45.6/5) | $H_2O$ | $H_2O$ | 195 | 0.57 | 73.0 | DCMD 3% NaCl $T_f$ = 80°C $T_p$ = 25°C | 10.5 |
| | | | $H_2O$ | DMAc/$H_2O$ (20/80)* | 160 | 0.48 | 75.7 | | 8.5 |
| | | | $H_2O$ | DMAc/$H_2O$ (40/60)* | 157 | 0.45 | 78.6 | | 7.5 |
| | | | $H_2O$ | DMAc/$H_2O$ (60/40)* | 158 | 0.39 | 73.5 | | 11.0 |
| | | | DMAc/$H_2O$ (50/50) | DMAc/$H_2O$* (50/50) | 67 | 0.77 | 83.3 | | 19.5 |
| Tang et al. [37] | NIPS | PVDF/DMAc/PEG/LiCl (13.0/79.2/5.2/2.6) | $H_2O$ | $H_2O$ | 200 | 0.14 | 79.2 | DCMD 9% NaCl $T_f$ = 65°C $T_p$ = 20°C | 16 |
| | | PVDF/DMAc/PEG/LiCl (17.0/72.8/6.8/3.4) | | | 215 | 0.38 | 68.6 | | 10 |
| Wang et al. [53] | NIPS | PVDF/NMP/EG (12/80/8) | NMP/$H_2O$ (80/20) | $H_2O$ | 110 | 0.15-0.18 | 73.8 | DCMD 3.5% NaCl $T_f$ = 80°C $T_p$ = 17.5°C | 41.5 |
| | | PVDF/NMP (12/88) | | | 110 | - | 68.5 | | 9 |
| Yao et al. [54] | NIPS | PVDF/TEP (11/89) | $H_2O$ | $H_2O$ | 175 | 0.048 | 81.8 | DCMD 7% NaCl $T_f$ = 60°C $T_p$ = 20°C | 14.9 |
| | | PVDF/TEP/Acetone (11/80.1/8.9) | | | 168 | 0.040 | 80.5 | | 13 |
| | | PVDF/TEP/Acetone (11/71.2/17.8) | | | 155 | 0.026 | 78.5 | | 11.4 |
| | | PVDF/TEP/Toluene (11/80.1/8.9) | | | 180 | 0.077 | 83.2 | | 16.5 |
| | | PVDF/TEP/Toluene (11/71.2/17.8) | | | 190 | 0.081 | 86.2 | | 18.9 |
| Wu et al. [55] | NIPS | PVDF/NMP/Glycerol (15/75/10) | EtOH/$H_2O$ (10/90) | EtOH/$H_2O$ (10/90) | 204 | - | 87.3 | DCMD 5% NaCl $T_f$ = 60°C $T_p$ = 17°C | 11.9 |
| | | PVDF/PVDF-HFP/NMP/Glycerol (13.5/1.5/75/10) | | | 216 | - | 83.3 | | 9.1 |

| | | | | | | | | |
|---|---|---|---|---|---|---|---|---|
| | | PVDF/PVDF-HFP/NMP/Glycerol (12/3/75/10) | | | 189 | - | 81.9 | | 8.9 |
| | | PVDF/PVDF-HFP/NMP/Glycerol (10.5/4.5/75/10) | | | 199 | - | 75.3 | | 6 |
| García-Fernández et al. [58] | | PVDF-HFP/DMF/TMP/PEG6000 (19/45.6/30.4/5) | $H_2O$ | $H_2O$ | 141 | | 67.3 | DCMD 3% NaCl $T_f$ = 80°C $T_p$ = 25°C | 32.0 |
| | | PVDF-HFP/DMAc/PEG6000 (19/76/5) | | | 150 | | 72.5 | | 54.0 |
| | | PVDF-HFP/DMAc/TMP/PEG6000 (19/45.6/30.4/5) | | | 113 | | 65.1 | | 50.0 |
| | | PVDF-HFP/DMAc/TMP/PEG6000 (19/30.4/45.6/5) | | | 180 | | 70.9 | | 68.4 |
| Huo et al. [60] | NIPS | PVDF/DMAc (12/88) | $H_2O$ | $H_2O$ | 130 | 0.35-0.40 | 68.7 | DCMD 3.5% NaCl $T_f$ = 80°C $T_p$ = 20°C | 10 |
| | | PVDF/DMAc/PEG1500 (12/83/5) | | | 130 | 0.50-0.60 | 72.4 | | 31 |
| | | PVDF/DMAc/LiCl (12/83/5) | | | 130 | 0.15-0.17 | 77.5 | | 22 |
| | | PVDF/DMAc/LiCl/PEG1500 (12/80/5/3) | | | 130 | 0.25-0.30 | 79.7 | | 41 |
| Simone et al. [61] | NIPS | PVDF/DMAc/$H_2O$ (20/74/6) | DMF/$H_2O$ (35/65) | $H_2O$ | 203 | 0.15 | 71.2 | VMD $H_2O$ $T_f$ = 50°C $P_v$ = 20 mbar | 4.3 |
| | | PVDF/DMAc/$H_2O$/PVP (20/68/6/6) | | | 184 | 0.16 | 74.5 | | 9.8 |
| | | PVDF/DMAc/$H_2O$/PVP (20/65/6/9) | | | 170 | 0.16 | 80.6 | | 17.9 |
| | | PVDF/DMAc/$H_2O$/PVP (20/63/6/11) | | | 211 | 0.18 | 81.5 | | 14.0 |
| | | PVDF/DMAc/$H_2O$/PVP 20/59/6/15) | | | 139 | 0.13 | 78.5 | | 15.3 |
| Garcia-Fernandez et al. [70] | NIPS | PVDF-HFP/DMAc/TMP/PEG (19/30.4/45.6/5) | $H_2O$ | $H_2O$ | 180 | 0.40 | 66.0 | DCMD 3% NaCl $T_f$ = 80°C $T_p$ = 25°C | 6.8 |
| | | | DMAc/$H_2O$ (20/80) | | 169 | 0.49 | 53.0 | | 8.1 |
| | | | DMAc/$H_2O$ | | 133 | 0.47 | 62.5 | | 7.8 |

| | | | | | | | | | |
|---|---|---|---|---|---|---|---|---|---|
| | | | (40/60) DMAc/$H_2O$ (50/50) | | 99 | 0.66 | 76.3 | | 12.6 |
| | | | DMAc/$H_2O$ (60/40) | | 96 | 0.71 | 78.4 | | 12.3 |
| Zhao et al. [90] | TIPS | PVDF/DMP (35/65) | DMP | $H_2O$ | 211 | 0.18 | 52 | DCMD 3.5% NaCl $T_f$ = 90°C $T_p$ = 20°C | 22 |
| Song et al. [91] | TIPS | PVDF/DOP/γ-BL (28/21.6/50.4) | Nitrogen | - | 205 | 0.24 | 66.8 | DCMD 3.5% NaCl $T_f$ = 90°C $T_p$ = 25°C | 23 |

* a triple orifice was used and the external coagulant was circulated through the outermost orifice of the spinneret.

TEP: Triethyl phosphate

DMP: Dimethyl phthalate

# 4. Mixed matrix hollow fibre membranes

Mixed matrix hollow fibres (MMHF) are membranes prepared by dispersing fillers such as nano-additives into the spinning polymer solution in order to improve some of the HF characteristics such as the hydrophobicity, mechanical properties, fouling or scaling resistance, thermal efficiency and in general the MD performance. The addition of nano-particles also modifies the coagulation mechanism during phase inversion, changing the HF membrane morphology and its properties [92].

For the preparation of mixed matrix HF membranes, dispersions with good stability are a key factor for improving the final membrane performance and its mechanical properties. Generally, three possible approach can be considered for the preparation of the spinning solution: i)- the filler is dispersed into the solvent with the aid of stirring and sonication if necessary, and the polymer is then added to the dispersion and finally dissolved; ii)- the filler is dispersed in a small amount of solvent while the polymer is dissolved in another container by means of the same solvent type, and both are finally mixed under stirring until the spinning solution becomes homogeneous, iii)- the filler is added directly inside the already prepared spinning solution. The first two methods are the most followed since they guarantee the best distribution of the filler inside the polymer matrix, reducing the risk of agglomeration and maximising the dispersion stability [93,94]. Mixed matrix membranes have been widely studied for gas separation applications [93,95] and water treatment by pressure driven membrane processes [96–99], but only recently have been proposed for MD. However, the majority of the published research studies are focused on flat sheet membranes while the addition of fillers in MD hollow fibre polymeric matrix is a field that has not been deeply investigated yet and only few works are currently available.

## *4.1. Materials for mixed matrix hollow fibre membranes*

### *4.1.1. Inorganic particles*

Particles and nanoparticles have been explored in membrane preparation with different aims, for example to enhance the membrane surface roughness, the hydrophobic character and to reduce the risk of membrane pore wetting. Hou et al. [100] investigated the effect of hydrophobic $CaCO_3$ nanoparticles on the morphology of PVDF HF membrane and its DCMD performance. Up on the addition of $CaCO_3$ nanoparticles, it was observed a decrease of the mean pore size with a narrow distribution and an increase of both the surface roughness and overall porosity. However, the DCMD permeate flux was increased but only for a limited concentration of $CaCO_3$ nanoparticles in the spinning solution (20 wt% respect to PVDF). Over this value, the porosity and pore size were decreased and further addition of $CaCO_3$ nanoparticles reduced the

DCMD flux. Compared to the unfilled PVDF HF membrane, the $CaCO_3$ mixed matrix PVDF HF membranes exhibited stable permeate flux and salt rejection factor during long-term application (30 days).

Zhang et al. [101] added hydrophobic silica ($SiO_2$) nanoparticles to PVDF, DMAC/TEP solution, then it was mixed with polydimethylsiloxane (PDMS) and tetraethoxysilane/tetrahydrofuran (TEOS/THF) solution in order to improve the miscibility of the two polymeric phases. The increase of the $SiO_2$ content improved the mechanical properties of the HF membrane and its hydrophobicity (i.e. the water contact angle was slightly enhanced from almost 90° of the PVDF/PDMS membrane up to 98° with the highest tested $SiO_2$ amount). However, the overall porosity was decreased up on the addition of $SiO_2$ whereas the outer surface presented larger pores for higher $SiO_2$ content. It must be noted that at the highest $SiO_2$ concentration (8.3 wt% respect to PVDF), some defects were formed preventing the use of the HF membrane in VMD.

Nano clays are an important category of fillers commonly used for nanocomposite production. The presence of ions between the lamellae of the silicate structure allows their modification opening this way the range of possibilities in membrane modification research. For this reason, nano clays effect on membrane performance has been investigated in various research studies [102–105]. As stated earlier, one of the major concerns of nanocomposite membrane preparation is the dispersion of the nanoparticles in dope solutions. The use of compatibilized nanoclays allows the polymer to enter between the galleries of nano clays exfoliating their lamellar structure and obtaining as a consequence an optimal distribution of the nanofillers in the dope solution.

Wang et al. [104] used a commercial hydrophobic clay (Cloisite® 20A) to improve the HF mechanical properties and obtain a nano porous membrane structure. These characteristics resulted in a peculiar cross section morphology with a sponge-like structure in the centre surrounded by two macrovoid layers. This morphology allowed an improvement of the thermal efficiency of the membrane and an increased permeability with a more stable DCMD performance. Moreover, the small dimension of the pores improved the rejection factor when using 3.5 wt% NaCl aqueous solution as feed, reaching a total salt rejection.

The clay loading is the primary factor investigated to prepare an optimised mixed matrix membrane. This must be enough to improve the MD performance without generating any defects. Mokhtar et al. [103,105] evaluated the effect of different nanofiller loadings on the structure and performance of PVDF HF membrane using differently modified hydrophobic nano clay (Cloisite® 15A). By adding small quantities of nanoparticles (3 wt% respect with the PVDF amount), the HF membrane performance was improved, but further increase of nanoparticles content led first to a decrease of the membrane permeability (5 wt%), and then to a reduction of the rejection factor of the membrane caused by defects and pore wetting (10 wt%). However, a DCMD permeate flux decrease about 50% was recorded when treating a textile wastewater for 40 h, because of fouling phenomena [106].

A new type of nano-additives that can be explored in mixed matrix HF membrane preparation are the metal-organic-frameworks (MOFs). These are formed by metal ions that are connected by organic ligands

creating a porous cluster structure [107]. MOFs can be tailored in order to obtain the desired structure and pore size [108] as well as the needed thermal stability, opening a wide field for advanced membrane development.

Cheng et al. [109] used aluminum fumarate MOFs to increase HF membrane permeability and its hydrophobicity. The aluminium MOFs were selected because of their easy preparation and stability in the saline aqueous media. The addition of MOFs in the spinning solution increased the pore size and porosity of the membrane, but above a certain concentration (1 wt%), their aggregation resulted in a reduction of porosity and DCMD permeate flux.

The HF membrane matrix prepared by TIPS technique can also be modified by introducing additives that promote or hinder polymer crystallization. Nucleating agents like PTFE or $CaCO_3$ were used to promote the nucleation of the polymer while the second category, comprising various amorphous polymers, can hinder the formation of crystal nuclei and suppress the crystallization process [90,110]. Song et al. [91] studied the effect of $CaCO_3$ particles on the performance of PVDF HF membranes. The addition of this inorganic filler resulted in an increase of the number of nucleating sites and improved the porosity and hydrophobicity of the HF membrane. However, the HF membrane performance decreased when using $CaCO_3$ concentrations greater than 2 wt% of the PVDF amount. In fact, the DCMD permeate flux was first increased from 23 kg/m$^2$h to 64 kg/m$^2$h when $CaCO_3$ amount was raised from 0 to 2 wt%, but a further increase up to 8 wt% resulted in a decrease of the DCMD permeate flux (31 kg/m$^2$h).

### *4.1.2. Carbon based fillers*

Different types of carbon-based additives have been tested for HF membrane preparation. These include activated carbon (AC), graphene, graphene oxide (GO) and carbon nanotubes (CNTs). Graphene can be easily dispersed into the spun polymeric matrix. This characteristic allows to use even high amounts of this filler in the spinning solution without the formation of defects in the HF membrane structure. Graphene was also found to be effective in increasing the pore size, preventing the wetting of the HF membrane pores, decreasing the fouling phenomena and enhancing the DCMD permeate flux stability during long time operation [111].

Zhao et al. [112] added activated carbon in the spinning polymer solution with different concentrations. The unfilled membrane showed a constant decline of the permeate flux. AC was found to increase HF membrane porosity, surface roughness and VMD membrane performance stability (i.e. increase of the permeate flux while the salt rejection factor was maintained stable). The addition of AC hindered wetting of membrane pores. However, the addition of larger quantities of AC (higher than 0.09 wt%), had a negative effect on the membrane porosity, on its roughness and decreased the VMD performance. These effects can be related to the agglomeration of the AC additive (shown in Figure 12) and the increase of the spinning solution viscosity.

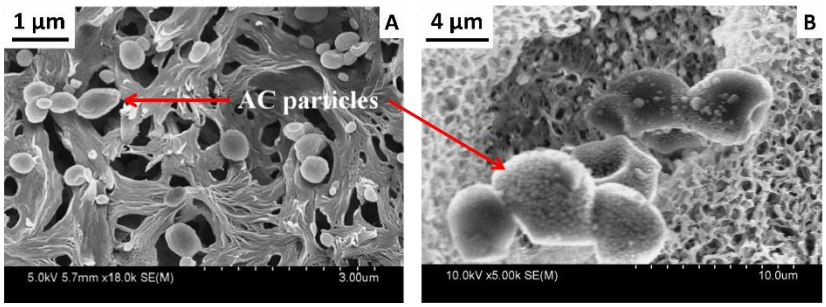


*Figure 12: (A) dispersion of AC additive in the HF membrane and (B) agglomeration at high concentration. Adapted from* [112].

Graphene oxide (GO) has been widely investigated for the preparation of HF membranes because of its easy and inexpensive production and interesting physical properties similar to those of graphene [113]. However, in contrast to graphene, GO has a large number of hydroxyl groups on its surface and, as consequence, a more hydrophilic character [114]. Interestingly, these hydroxyl groups can be functionalised obtaining nano-additives that can increase both the mechanical properties and hydrophobicity of the HF fibre membranes. Moreover, the functionalising agents can be selected in order to tune the affinity of GO with the hosting polymer improving the dispersion of the GO nano-sheets in the polymeric matrix [115]. Lu et al. [116] treated GO using n-butylamine and investigated the effect of its concentration on the HF membrane structure and MD performance. In fact, alkylamines can react with the epoxy and carboxylic groups of GO, increasing its water contact angle. Provided that GO nano-sheets act as nucleation spots during phase inversion, increasing GO content induces the formation of more spherulites with small size.

The increase of the modified GO concentration resulted in an enhancement of the solution viscosity that changed the cross section morphology of the HF. As the GO content was increased, the overall porosity was enhanced and reached 89% when 1.5 wt% (respect to the polymer amount) was added. However, the higher solution viscosity reduced the outer surface pore size and porosity. This second effect outweighed the increase of the overall porosity and the DCMD performance (3.5 wt% NaCl, $T_f$ = 60°C, $T_p$ = 16°C) showing a decrease of the permeate flux, from 30.6 kg/m$^2$h to 24.8 kg/m$^2$h as the GO content was increased from 0 to 1.5 wt%.

Carbon nanotubes (CNTs) are another interesting carbon-based filler used to prepare mixed matrix HF membranes. The production techniques of these nano-additives progressed rapidly during last decade allowing cost-effective preparation procedures and CNTs of various geometries [117]. It has been demonstrated that water transport through CNTs is orders of magnitude faster than in other porous materials because of the regular and smooth structure of the inner channel [118]. Therefore, CNTs may offer supplementary paths for water molecules diffusion through the membrane and enhance the overall mass transfer coefficient [119]. Moreover, the addition of CNTs improves the mechanical properties and stability of the polymer matrix [120]. Balis et al. [121] prepared multi wall carbon nanotubes (MWNTs) by means of

chemical vapour deposition technique, which allowed high yields and low production costs. MWNTs were added to two different spinning solutions, PVDF and PVDF-HFP, and their effects on membrane morphology and performance were investigated. Both MWNTs mixed matrix PVDF and PVDF-HFP HF were thinner with a cross section containing wider and longer macrovoids compared with the unfilled HF membranes. This effect was found to be more relevant for PVDF-HFP HF membrane with higher overall porosity compared with PVDF HF membrane.

#### *4.1.3. Other particles*

Zhao et al. [90] prepared PVDF HF membranes by TIPS technique using PTFE particles. It was found that the addition of PTFE particles in the PVDF spinning solution increased the number of spherulites and reduced their dimension. The larger number of small spherulites is associated to smaller pore size with narrower distribution. Moreover, because the PTFE intrinsic hydrophobicity, the water contact angle of the PVDF HF membrane was increased from 94° to 106° and the mechanical properties were enhanced after adding PTFE particles. In general, it was found that the DCMD permeate flux was in concordance with the porosity. For a PTFE content higher than 1 wt%, both the porosity and the DCMD permeate flux were reduced. The mixed matrix HF membrane prepared with 1 wt% PTFE exhibited the highest permeate flux. It was claimed that the PTFE mixed matrix HF membrane exhibited an improved wetting resistance and stable permeate flux together with a good salt rejection factor over 50 h DCMD operation.

### *4.2. Thermal efficiency of mixed matrix hollow fibre membranes*

The introduction of fillers into polymeric membrane matrix can modify the thermal conductivity coefficient of the membrane and the permeate flux together with the thermal efficiency of the process as consequence. It was found that the addition of fillers with high thermal conductivity (e.g. carbon nanotubes) reduced the thermal efficiency of the MD process because of the increase of the thermal conductivity of the membrane [121,122]. However, this effect can be mitigated by the enhancement of the permeate flux that increased the heat transfer associated to mass transfer respect to the heat loss by conduction through the membrane [100].

As stated earlier, another parameter affecting the thermal efficiency of MD process is the membrane void volume fraction or porosity. In fact, the gases entrapped inside the pores reduce the heat transfer by conduction because the thermal conductivity of gases is an order of magnitude smaller than that of the membrane matrix. As described in the previous paragraph and summarized in Table 2, the addition of fillers commonly enhances membrane porosity and the MD permeate flux resulting in a greater thermal efficiency [109]. However, the addition of MWNTs in PVDF and PVDF-HFP had different effects on the thermal efficiency of HF membranes used in DCMD [121]. For PVDF-HFP, the MWNTs were concentrated in the inner sponge

layer of the HF membrane brought into contact with the cold permeate and had a positive effect on the thermal efficiency through the reduction of the temperature polarisation effect increasing therefore the permeate flux. The effect was completely opposite for PVDF polymer. The MWNTs were concentrated in the external layer of the HF membrane and brought in contact with the hot feed solution and had a negative influence on the thermal efficiency, despite increasing the permeate flux.

### *4.3. Remarks and future directions on mixed matrix hollow fibre membranes*

Table 2 summarizes the main spinning parameters of mixed matrix HF membranes used in MD together with their characteristics discussed in this section. Some data that were not directly available in the papers have been extrapolated from the graphs using Quintessa© Graph Grabber 2.2 software. The addition of fillers offers numerous opportunities to improve the membrane performance. In fact, by considering different kind of fillers it is possible to tune various aspects of the membrane structure, such as their porosity and hydrophobicity. For instance, the addition of fillers in the spinning solution can modify the coagulation mechanism during phase separation process generating different structures.

One of the key parameters for the preparation of mixed matrix HF membranes is the amount of the filler in the spinning solution. It has been confirmed in majority of research studies [90,91,100,103,109] that there is a critical value of filler content in a given spinning solution at which the membrane performance is maximised. Generally, this value coincides with the highest filler concentration at which a complete dispersion can be obtained. Increasing further the filler content, above this critical value, leads to a worse dispersion and a gradual reduction of both porosity and MD permeate flux, and in some cases also results in the reduction of the salt rejection factor due to pore wetting associated to the presence of defects in the membrane matrix.

The improvement of the permeate flux and the increase of the porosity achieved by the addition of fillers, has also a positive effect on the thermal efficiency of the MD process, especially at high feed temperatures. On the other hand, the addition of the fillers in the membrane matrix may increase the thermal conductivity of the membrane and the subsequent heat loss due to heat transfer by conduction through the membrane mixed matrix [121,122].

It must be noted that the application of fillers, including nano-additives such as nano-particles, in HF membrane engineering for MD has not been deeply investigated. The use of low thermal conductivity fillers may be an interesting subject to explore in order to improve the MD performance of mixed matrix HF membranes. The availability of a large choice of possible fillers, as well as the possibility to perform different types of surface modification procedures, offers numerous opportunities for investigation in this specific field.

*Table 2: Spinning conditions and performance of mixed matrix hollow fibres used in MD.*

| Ref. | Technique | Dope solution composition (wt%) | BF | ECB | Thickness (μm) | Pore size (μm) | Porosity (%) | MD conditions | Permeate flux (kg/m²h) |
|---|---|---|---|---|---|---|---|---|---|
| Hou et al. [100] | NIPS | PVDF/DMAc/PEG/LiCl (12/80/3/5) | $H_2O$ | $H_2O$ | 130 | 0.32 | 79.8 | DCMD 3.5% NaCl $T_f$ = 80°C $T_p$ = 20°C | 40.5 |
| | | PVDF/DMAc/PEG/LiCl/$CaCO_3$ (12/78.8/3/5/1.2) | | | 150 | 0.29 | 81.5 | | 42.5 |
| | | PVDF/DMAc/PEG/LiCl/$CaCO_3$ (12/77.6/3/5/2.4) | | | 150 | 0.25 | 85.3 | | 46.4 |
| | | PVDF/DMAc/PEG/LiCl/$CaCO_3$ (12/76.4/3/5/3.6) | | | 150 | 0.18 | 82.6 | | 39.0 |
| | | PVDF/DMAc/PEG/LiCl/$CaCO_3$ (12/75.2/3/5/4.8) | | | 150 | 0.10 | 78.7 | | 30 |
| | | PVDF/DMAc/PEG/LiCl/$CaCO_3$ (12/74/3/5/6) | | | 150 | 0.04 | 73.3 | | 22.7 |
| Wang et al. [104] | NIPS | PVDF/NMP/EG (10.0/78.0/12.0) | $H_2O$ | $H_2O$ | 160 | | 89.6 | DCMD 3.5% NaCl $T_f$ = 81.5°C $T_p$ = 17.5°C | 83.8 |
| | | PVDF/NMP/EG/Cloisite 20A (10.0/74.7/12.0/3.3) | | | 180 | | 86.7 | | 79.2 |
| Mokhtar et al. [103] | NIPS | PVDF/NMP/EG (12/80/8) | NMP/$H_2O$ (80/20) | $H_2O$ | 144 | 0.044 | 82.7 | DCMD 0.05% Reactive black 5 $T_f$ = 90°C $T_p$ = 20°C | 6.4 |
| | | PVDF/NMP/EG/Cloisite 15A (11.9/79.7/8.0/0.4) | | | 127 | 0.088 | 83.7 | | 15.2 |
| | | PVDF/NMP/EG/Cloisite 15A (11.9/79.5/8/0.6) | | | 132 | 0.108 | 83.0 | | 6.3 |
| | | PVDF/NMP/EG/Cloisite 15A (11.8/79.1/7.9/1.2) | | | 132 | 0.144 | 83.0 | | 6.4 |
| Cheng et al. [109] | NIPS | PVDF/DMAc/PG (16.5/61.5/22) | $H_2O$ | $H_2O$ | 195 | 0.233 | 70.6 | DCMD 1% NaCl $T_f$ = 60°C $T_p$ = 20°C | 5.4 |
| | | PVDF/DMAc/PG/AlFu MOF (16.5/61.4/22.0/0.1) | | | | 0.264 | 76.4 | | 6.8 |

| | | | | | | | | | |
|---|---|---|---|---|---|---|---|---|---|
| | | PVDF/DMAc/PG/AlFu MOF (16.4/61.4/22.0/0.2) | | | | 0.294 | 88.4 | | 10.4 |
| | | PVDF/DMAc/PG/AlFu MOF (16.4/61.3/21.90/0.3) | | | | 0.291 | 84.1 | | 8.4 |
| | | PVDF/DMAc/PG/AlFu MOF (16.4/61.2/21.9/0.5) | | | | 0.290 | 82.7 | | 7.8 |
| | | PVDF/DMAc/PG/AlFu MOF (16.4/61.1/21.9/0.7) | | | | 0.281 | 77.8 | | 6.6 |
| | | PVDF/DMAc/PG/AlFu MOF (16.4/61.0/21.8/0.8) | | | | 0.279 | 76.2 | | 5.3 |
| Zhao et al. [112] | NIPS | PVDF/PG/DMAc (16/22/62) | $H_2O$ | $H_2O$ | - | 0.287 (max) | 80 | VMD 10% NaCl $T_f$ = 70°C $P_v$ = 200 mbar | 42 |
| | | PVDF/PG/DMAc/AC (16/22/62/0.09) | | | - | 0.285 (max) | 90 | | 54.9 |
| Lu et al. [116] | NIPS | PVDF/PTFE/EG/NMP (10/3/12/75) | $H_2O$ | IPA/$H_2O$ (60/40) | 126 | 0.081 | 68.9 | DCMD 3.5% NaCl $T_f$ = 80°C $T_p$ = 20°C | 30.6 |
| | | PVDF/PTFE/EG/NMP/GO (10/3/12/74.9/0.06) | | | 123 | 0.063 | 76.8 | | 28.2 |
| | | PVDF/PTFE/EG/NMP/GO (10/3/12/74.9/0.13) | | | 121 | 0.062 | 88.1 | | 26.1 |
| | | PVDF/PTFE/EG/NMP/GO (10/3/12/74.8/0.19) | | | 108 | 0.049 | 88.9 | | 24.8 |
| | | PVDF/PTFE/EG/NMP/GO (10/3/12/74.8/0.26) | | | 122 | 0.042 | 94.9 | | - |
| Balis et al. [121] | NIPS | PVDF/NMP (19/81) | NMP/$H_2O$ (80/20) | $H_2O$ | 241 | 0.438 | 69.1 | DCMD 3% NaCl $T_f$ = 75°C $T_p$ ≈ 60°C | 0.6 |
| | | PVDF/NMP/MWNT (19/80.8/0.2) | | | 161 | 0.422 | 69.6 | | 1.1 |
| | | PVDF-HFP/NMP (30/70) | | | 258 | 0.183 | 53.1 | | 0.4 |
| | | PVDF-HFP/NMP/MWNT (29.9/69.8/0.3) | | | 173 | 0.250 | 60.6 | | 0.8 |
| Zhao et al. [90] | TIPS | PVDF/DMP (35/65) | DMP | - | 211 | 0.18 | 52 | DCMD 3.5% NaCl $T_f$ = 90°C | 22 |
| | | PVDF/DMP/PTFE | | | 234 | 0.10 | 65 | | 81 |

| | | | | | | | | | |
|---|---|---|---|---|---|---|---|---|---|
| | | (34/65/1) | | | | | | $T_p$ = 20°C | |
| | | PVDF/DMP/PTFE (33/65/2) | | | 224 | 0.08 | 62 | | 52 |
| | | PVDF/DMP/PTFE (30/65/5) | | | 224 | 0.12 | 58 | | 39 |
| Song et al. [91] | TIPS | PVDF/DOP/γ-BL (28/21.6/50.4) | Nitrogen | - | 205 | 0.24 | 66.8 | DCMD 3.5% NaCl $T_f$ = 90°C $T_p$ = 25°C | 23 |
| | | PVDF/DOP/γ-BL/$CaCO_3$ (28/21.5/50.2/0.3) | | | 215 | 0.26 | 68.5 | | 41 |
| | | PVDF/DOP/γ-BL/$CaCO_3$ (28/21.4/50/0.6) | | | 219 | 0.28 | 69.7 | | 64 |
| | | PVDF/DOP/γ-BL/$CaCO_3$ (28/21.3/49.8/0.8) | | | 212 | 0.27 | 69.1 | | 55 |
| | | PVDF/DOP/γ-BL/$CaCO_3$ (28/21.2/49.4/1.4) | | | 205 | 0.26 | 68.2 | | 45 |

PG: propylene glycol

AlFu MOF: Aluminium fumarate metal-organic-framework

# 5. Dual layer hollow fibre membranes

Inspired by double layered flat-sheet hydrophobic/hydrophilic membranes, consisting of a thin hydrophobic layer with small pore size supported on a thicker hydrophilic layer with larger pore size [123–125], dual layer hollow fibres (DLHF) were proposed to increase the DCMD permeate flux and reduce the heat transfer by conduction increasing the thermal efficiency of the MD process. In this case, liquid permeate penetrates inside the bigger pores of the hydrophilic layer reducing the distance between the liquid/vapour interfaces formed at both sides of the hydrophobic layer and an increase of the permeate flux is expected, while thicker hydrophilic layer reduces the heat transfer by conduction and provides the needed mechanical properties [126–128].

DLHF membranes are mainly prepared by simultaneous co-extrusion of two polymer dope solutions using a triple-orifice (or quadruple-orifice) spinneret. Different bore fluids and external coagulants were investigated to obtain the desired morphologies via NIPS technique. Surface modified HF was also proposed using host hydrophilic polymers such as polyetherimide (PEI) and low surface energy additives such as fluorinated polyurethane additives (FPA) that can migrate towards the inner surface, outer surface of both forming layered HF membranes by NIPS technique [50]. To the best of our knowledge, up to date TIPS technique is not used for the preparation of DLHF.

DLHF can be made using two different polymers or the same polymer. When using two different materials, their compatibility plays a fundamental role in order to avoid any possible delamination of the two layers. The two layers must undergo similar solidification conditions and shrinkage ratio. In fact, one of the major problems in DLHF preparation is the delamination phenomenon of the formed two layers. Figure 13 shows the possible evolution of the membrane structure on the basis of the shrinkage ratio of both layers.

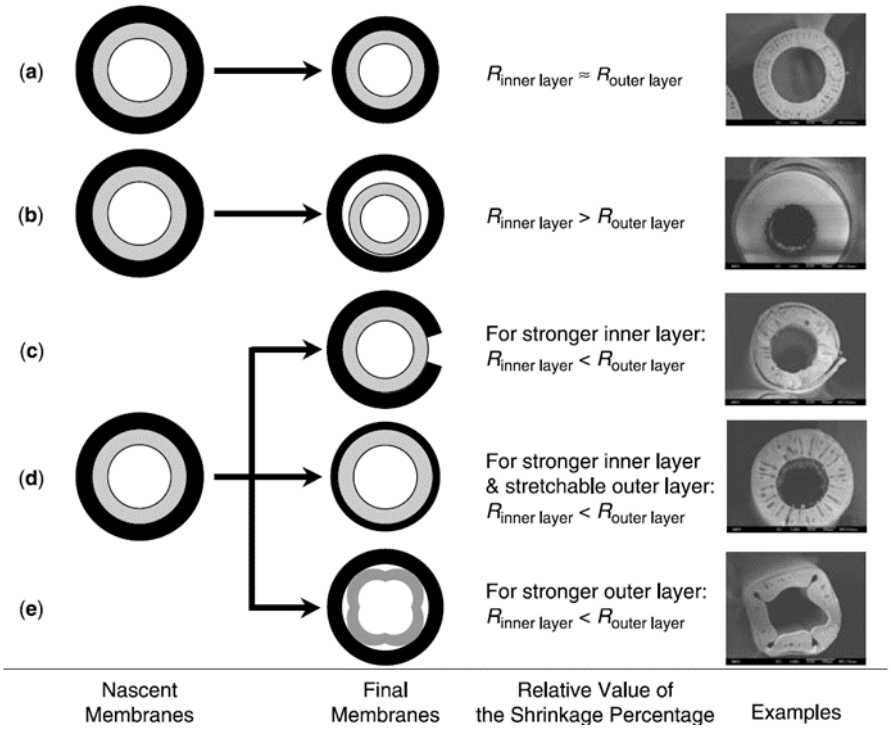


*Figure 13: Schematic diagram of the influence of shrinkage percentage on dual layer hollow fibre structure. Adapted from* [129].

Good delamination-free membranes were obtained when using polymers with similar shrinkage factors (Figure 13a) or for low contracted inner layer and more stretchable external polymer (Figure 13d). Complete delamination happened when the inner layer shrunk more than the outer one (Figure 13b), whereas the opposite situation (i.e. the outer layer contracted more than the inner one) led to the break of the weak selective layer (Figure 13c) or lumen geometry collapse (Figure 13e) when the outer layer was stronger than the inner one.

Li et al. [129] studied the effect of various parameters on the adhesion of the two layers. By increasing the inner dope solution flow rate, it was possible to eliminate the delamination. In fact, using a higher inner dope solution flow rate, a thicker layer was created and solidification was slower creating lower shrinkage. Another explored way to prepare a delamination free membrane is using a weak BF that reduces the coagulation rate. A similar approach was followed by Setiawan et al. [130], who studied the effect of various parameters on the adhesion of the two layers. One of the main phenomena affecting delamination is the diffusion rate in the two formed layers. When the nonsolvent diffusion rate in the outer layer is higher than in the inner one, the coagulant accumulates inside the void volume (e.g. finger-like structure) of the external layer and hinders the linking between the two layers, favouring delamination effects. Instead, if the diffusion of nonsolvent is slower in the outer layer than in the inner one, a good adhesion is obtained. However, in this case a higher expansion of the inner layer, caused by the formation of macrovoids, can lead to a deformation of the HF lumen.

Other factors that promote the adhesion of the two layers and reduce the risk of delamination are the air gap distance (i.e. as it is increased, the polymer solutions have more time to go inter-diffusion and create

more linking spots forming a denser surface on the external layer that reduces the coagulation rate when the fibre is immersed in the ECB [130,131]); the spinning solutions temperature (i.e. higher temperatures reduce the polymer solutions viscosities and enhance the chain mobility favouring the interdiffusion between the two layers [132]); the use of weak coagulants (i.e. weak coagulants increase adhesion of the two layers by slowing the precipitation effect [129,130,133]); and the higher inner dope solution concentration (i.e. polymer solutions with low concentrations tend to have a higher shrinkage factor resulting in a more severe delamination effect [129,132,134]).

The choice of adequate materials to prepare DLHF membranes plays a major role in obtaining delamination free structure. In fact, using thermodynamically compatible solutions helps creating a stable interface between the two layers because the main components of the two dope solutions tend to diffuse into each other producing a well interconnected interface [129,135].

It is worth quoting that DLHF membranes have been widely studied in other membrane separation processes such as pervaporation [136–138], forward osmosis [139–141] and gas separation [134,142–145], as well as in membrane catalytic reactors [146–148].

### *5.1. Spinneret design*

For the preparation of dual layer HF, triple-orifice spinnerets are commonly employed. The inner channel consists on a needle for the circulation of the BF, while the two polymer solutions flow through the middle and external annular gaps. One of the main characteristics of this spinneret design is the size of the three different orifices. Narrower gaps induce higher shear rate in the spinning solution and therefore a higher orientation of the polymer macromolecules [76,149]. This results in tighter packing of the HF structure and higher membrane rejection factors [143].

For DLHF membrane engineering, one of the main tasks is to ensure a good interaction between the two layers in order to avoid any possible delamination. To address this problem some research studies [131,143,150] suggest the use of spinnerets with a premixing section (i.e. the spinneret walls between the two dope solutions are interrupted before the exit of the spinneret) (Figure 14). This design permits the interdiffusion of the two spinning polymeric solutions and favours a better binding of the two forming layers.

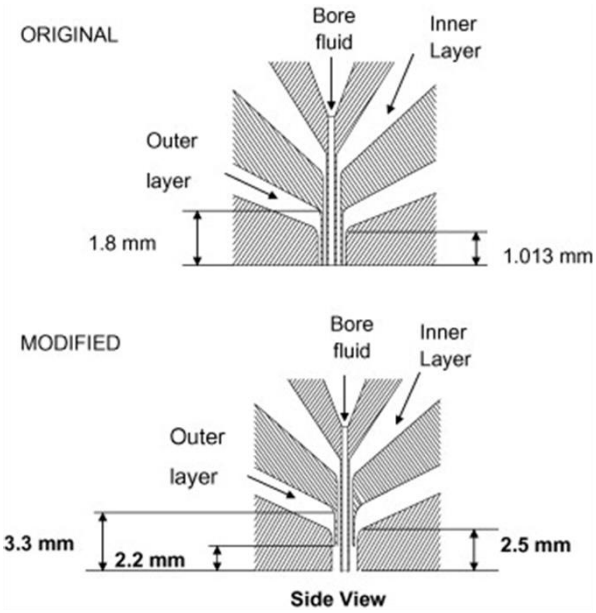


*Figure 14: Original and modified dual layer spinneret designs. Adapted from* [150].

Another common problem is related to the irregular distribution of the spinning solution through the spinneret lumen. This can create inhomogeneities in the spinning solution flow and in the thickness of the membrane layers. Li et al. [151] suggested the use of a modified spinneret including an annular distributor in order to obtain a better distribution of the spinning solution and more uniform membrane layers (Figure 15).

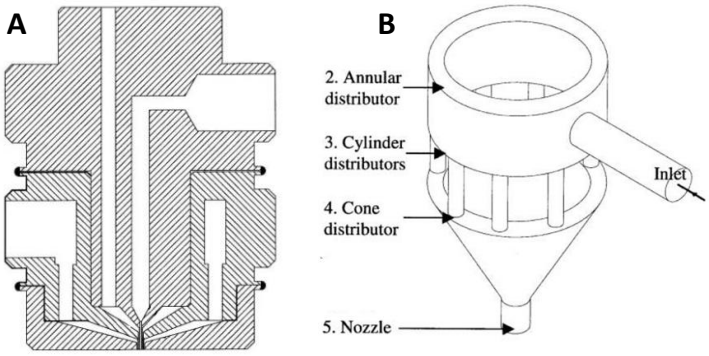


*Figure 15: Structure of (A) dual layer spinneret, (B) outer passage of dual layer spinneret. Adapted from* [151].

Using a weak nonsolvent both as BF or ECB can promote the formation of highly porous and hydrophobic membranes. To lower the strength of the nonsolvent it is common to use high concentrations of organic solvents or additives. At an industrial scale, this creates various problems both in terms of production costs and environmental concerns especially their use as ECB. Some researchers proposed the use of quadruple spinneret. Amaral et al. [145,152] tested the spinneret schematized in Figure 16. The most external channel is fed with a weak nonsolvent, which initiates the polymer coagulation as soon as it exits the spinneret. Using small volumes of weak nonsolvent allows to obtain a defect free outer layer with a good adhesion with the inner one.

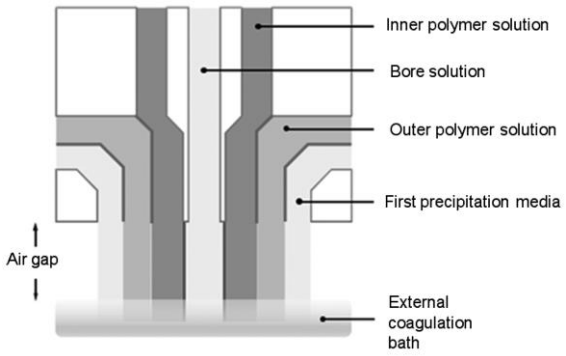


*Figure 16: Quadruple-orifice spinneret scheme. Adapted from* [145].

In order to prepare DLHF membranes, three approaches have been considered: i) use of a hydrophobic polymer for the selective hydrophobic layer and a hydrophilic polymer acting as a support with triple or quadruple-orifice spinnerets (Figs. 13 and 14); ii) use of two spinning solutions of the same polymer but with different compositions and filler or modifier (Fig. 13), and iii) use of a fluorinated surface modifying additive and a hydrophilic hosting polymer with a traditional spinneret (i.e. single layer Fig. 2). In this last approach, the fluorinated surface modifying additive migrates to the surface of the host hydrophilic polymer layer rendering more hydrophobic. While the first method could theoretically allow to choose the best material for both layers, severe delamination problems were observed as reported earlier [132,153–156].

### *5.2. Spinning conditions*

The spinning conditions play a critical role in determining the DLHF structure and its properties as highlighted before for single layer hollow fibres. By modifying the spinning parameters, it is possible to tune the morphological structure of the different layers enhancing the MD performance of the final HF membrane.

#### *5.2.1. Use of different polymers for each layer*

Ding et al. [153] suggested that the dope composition of both spinning solutions used to prepare both inner and outer layers has to be adjusted in order to obtain similar precipitation rates for both layers. The outer layer was formed using 28 wt% polyimide (Matrimid® 5218) solution, while three different polymers (polysulfone, PSf; polyethersulfone, PES; and polyetherimide, PEI) were tested for the inner layer. When the inner solution had a similar precipitation rate to the outer one (PSf and PES), the interface between the two precipitation rates was characterised by large pores and the transmembrane gas flow was high. When using PEI, the inner solution coagulated faster than the outer solution and at the interface between the two layers a dense skin was formed. Similar results were obtained by changing the inner layer precipitation rate adding water to the solution (2 wt% and 7 wt%). In fact, the formation of an almost dense layer at the interface of the two layers was observed when the coagulation of the internal layer was fast due to the addition of nonsolvent ($H_2O$) in the spinning solution and to the high affinity of the solvent with the nonsolvent.

Zuo et al. [155] used two different polymers for the internal and external layers. PVDF was chosen to prepare the hydrophobic layer while polyetherimide (ULTEM®, PEI) was selected to prepare the hydrophilic layer because of its good mechanical properties and a similar solubility parameter (23.7 $MPa^{0.5}$) to PVDF (23.2 $MPa^{0.5}$). A lower polymer concentration of the outer spinning solution was used (i.e. 10 wt% PVDF outer solution and 12.5 wt% PEI inner solution) in order to induce a higher shrinkage of the outer layer compared to the inner one and prevent delamination of the two layers. Although weak nonsolvents were used as both BF (NMP/$H_2O$ 50/50) and ECB (isopropyl alcohol (IPA)/$H_2O$ 50/50), an almost dense fraction was formed at the interface between the two layers. This results in a low VMD permeate flux (2.4 $kg/m^2h$ at 60°C feed solution with a NaCl concentration of 3.5 wt%, and a vacuum pressure of 20 mbar). The addition of 15 wt% of $Al_2O_3$ nanoparticles in the inner spinning solution resulted in the creation of a porous structure in the outer surface of the inner layer, an increase of the VMD permeate flux (27.9 $kg/m^2h$ at 60°C feed solution with a NaCl concentration of 3.5 wt%, and a vacuum pressure of 20 mbar) and an improved Young's modulus, which was increased up to 279.5 MPa.

A particular procedure to prepare DLHF was proposed by Khayet et al. [50] using a fluorinated additive having lower surface energy than a host hydrophilic polymer, and therefore tends to migrate towards the polymer/air interface during HF spinning using a simple spinneret and following the same procedure to that of single layer HF spinning. A fixed amount (2 wt%) of fluorinated polyurethane (FPA) was added into the spinning solutions prepared with different concentrations of a host hydrophilic PEI (14 – 17 wt%). For sake of comparison, a single layer HF was prepared without FPA using 14 wt% PEI. The prepared HF had similar cross section morphologies characterised by two separate layers of finger-like structure and denser thin skin layers at the inner and outer surfaces. The increase of the PEI concentration in the spinning solution reduced the porosity and the pore size, whereas the *LEP* was increased. The X-ray energy dispersive (EDX) analysis highlighted higher fluorine content associated to FPA at the inner and outer layers than in the centre of the cross section. A greater amount of fluorine and F/C ratio was detected at the outer layer than at the inner one indicating the migration of FPA towards the external layer of the HF rendering it more hydrophobic. This result was confirmed by X-ray photoelectron spectroscopy (XPS) analysis. The segregation of the hydrophobic additive, FPA, improved the water contact angle of both the inner and the outer layers of the HF, but the outer layer was more hydrophobic than the inner layer (i.e. the water contact angle increased from 87.2° up to 132.7° for the outer surface and from 80.5° to 97.2° for the inner surface). The prepared HF membranes were subsequently tested in desalination by DCMD using as feed distilled water and two NaCl solutions (12 g/L and 30 g/L). Because of its most hydrophobic character, the feed solution was brought into contact with the outer layer. The membrane prepared without FPA showed low salt rejection factor, as the permeate electrical conductivity increased from 7.1 µS/cm to 101.5 µS/cm when 12 g/L NaCl solution was used as feed ($T_f$ = 80°C, $T_p$ = 20°C) because of its hydrophilic character. However, all modified HF membranes exhibited good salt rejection factors (>99.9%) and the one prepared with the lowest amount of PEI (14 wt%) showed

the highest DCMD permeate. During almost two months consecutive DCMD operation using 30 g/L NaCl solution ($T_f$ = 80°C, $T_p$ = 20°C), this modified HF membrane maintained a stable permeate flux (23.8 kg/m$^2$h) with a very high salt rejection factor (i.e. the electrical conductivity of the permeate was lower than 6 μS/cm).

### *5.2.2. Use of the same polymer for both layers*

The second considered approach to prepare DLHF have been applied using different compositions of the two spinning solutions prepared with the same polymer. This procedure maximises the interactions between the two layers and reduces the risk of mechanical failure. However, by using the same polymer it is not possible to produce a dual layered hydrophilic/hydrophobic HF membranes. The addition of modifiers or fillers including nano-additives was explored to prepare DLHF [100,127,157–163].

Nanoclays were the first developed nanofillers for polymer modification and one of their strength is the possibility of easily exchanging the interlamellar cations in order to tune their hydrophilicity [164]. For this reason, Bonyadi et al. [157] prepared dual layer hydrophobic/hydrophilic PVDF hollow fibres using two different commercial nanoclays, namely Cloisite® 15A, which is hydrophobic, and Cloisite® $Na^+$, which is hydrophilic. Adding 30 wt% (respect the PVDF polymer loading) of Cloisite® 15A in the external spinning solution a contact angle of 140° was achieved. Higher amounts were tested but resulted in brittle HF membranes and difficult spinning because of the spinneret blockage. The inner spinning solution was composed by a lower concentration of PVDF (8.5 wt%) than that of the outer spinning solution (12.5 wt%) and 4 wt% of polyacrylonitrile (PAN) with 50 wt% of Cloisite® $Na^+$. The authors claimed that the PAN acted as a linker between the PVDF and the hydrophilic nanoclay facilitating the dispersion of the nanoparticles in the spinning solution and stabilizing the formed HF membrane.

A further step on the use of nanoclays was performed by Su et al. [165], who also used Cloisite® 15A nanoclay to increase the external layer hydrophobicity (Figure 17 A and B) but incorporated multiwall carbon nanotubes and graphite particles in the inner layer in order to increase its thermal conductivity and reduce the temperature polarization effect. It was found that the MWNTs created a network connecting the polymers globules and the graphite particles (Figure 17 C) increasing more than ten times the original matrix thermal conductivity. This modification allowed to increase the DCMD permeate flux up to 66.9 kg/m$^2$h when using 3.5 wt% NaCl aqueous solution with a feed temperature ($T_f$ = 80°C) and a permeate temperature ($T_p$ = 15°C).

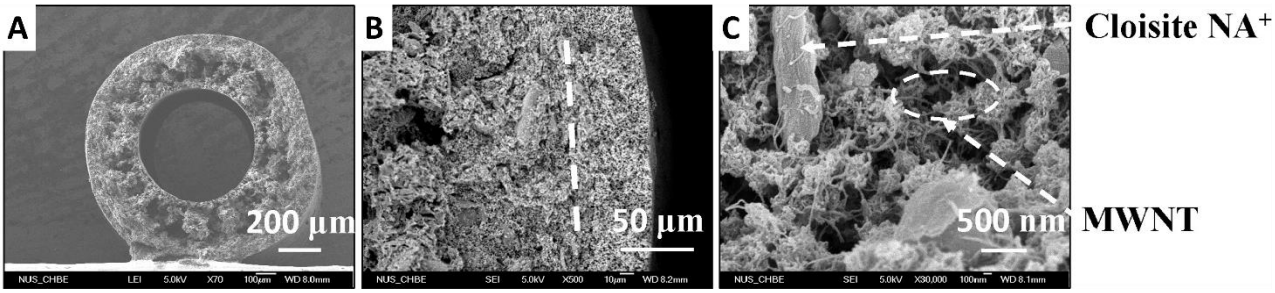


*Figure 17: Membrane with MWNT used as filler in the inner layer. (A) cross section; (B) outer layer; (C) inner layer. Adapted from* [165].

Another class of used nanofillers are the silica nanoparticles. Because of their surface hydroxyl groups, this type of nanoparticles is hydrophilic. However, many studies have been carried out on ceramic materials to render them hydrophobic. The main procedure is to substitute the hydroxyl groups with alkyl silanes [166] or fluoroalkyl silanes [167]. This kind of nanofiller was tested by Edwie et al. [158], who synthesized and modified silica nanoparticles with a fluoroalkyl silane. The modified filler was then added to the outer spinning solution in order to increase the hydrophobicity of the external layer, while ethylene glycol was used in the inner polymeric solution to reduce the mass transfer resistance of the internal layer. The morphology of the HF was not deeply influenced by the addition of 5 wt% of modified nanofillers. The cross section was characterised by a hydrophilic inner layer with macrovoids near the inner surface acting as a support for the thinner hydrophobic outer layer having a globular structure. The addition of fluorinated silica nanoparticles slightly increased the hydrophobicity of the outer layer (i.e. the contact angle increased from 136° to 140°) but had no effect on the wetting resistance of the HF membrane, probably because of unreacted surface hydroxyl groups. However, the pore size and porosity were reduced when the filler was added. This effect caused a reduction of the DCMD permeate flux from 83.4 kg/m$^2$h (feed: 3.5 wt% NaCl solution, $T_f$ = 80°C, $T_p$ = 17°C) in absence of silica particles to 77 kg/m$^2$h when 5 wt% of filler was added.

Apart from the inorganic particles, polymeric ones such as PTFE particles were also considered to increase the hydrophobic character of the outer layer of the DLHF membranes. Teoh et al. [159] studied the effect of PTFE particles both in single and double layered PVDF HF membranes. Adding different quantities of PTFE, between 20 and 40 wt% respect to PVDF amount, resulted in a decrease of the overall porosity of the HF membrane and in an increase of the hydrophobicity. These modifications affected the DCMD permeate flux that was reduced from 56.4 kg/m$^2$h registered for the lowest PTFE concentration (20 wt%) to 48.7 kg/m$^2$h when the highest amount of filler was added (feed: 3.5 wt% NaCl solution, $T_f$ = 80°C, $T_p$ = 17°C). For the single layer HF membrane, the PTFE particles were dispersed in all its cross section, but for the DLHF only its external selective layer was modified and therefore it was the only layer suffering the reduction of the porosity. These results were confirmed by Wang et al. [168], who prepared PVDF DLHF membranes using different spinning solutions by changing the dope composition and coagulant liquids in order to obtain an external hydrophobic layer containing PTFE particles with a sponge-like structure and a hydrophilic layer characterised by large finger-like macrovoids. Their work confirmed the better performance of the DLHF

respect to a SLHF prepared under similar spinning conditions. In fact, the DCMD permeate flux of SLHF was almost 50 L/m$^2$h while that of DLHF reached 99 L/m$^2$h under the same operating conditions (3.5 wt% NaCl aqueous solution with a feed temperature, $T_f$ = 80°C, and a permeate temperature, $T_p$ = 15°C). Moreover, by changing the flow rate of the inner spinning solution it was possible to control the thickness of the two layers (i.e. the decrease of the polymer flow rate results in a thinner external layer as shown in Figure 18).

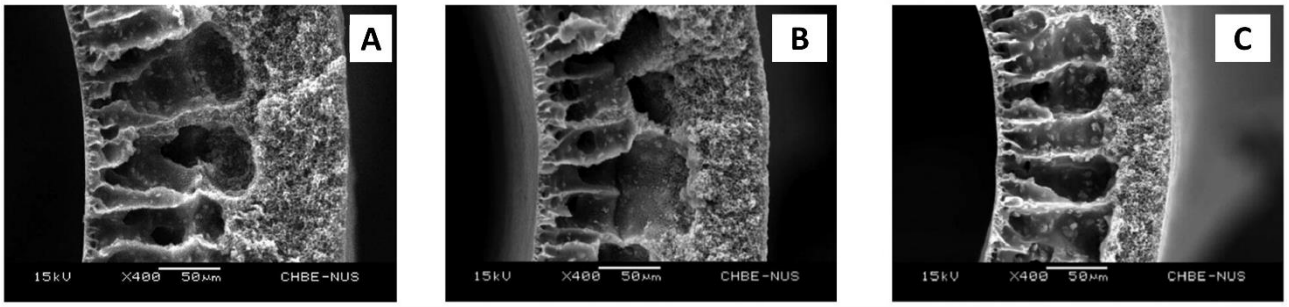


*Figure 18: Morphology of the cross sections of DLHF prepared with different inner solution flow rates: (A) 2 mL/min; (B) 1,6 mL/min; (C) 1,2 mL/min. Adapted from* [168].

### *5.2.3. Effect of spinning solution modifier*

The spinning solution composition plays a major role in determining the final membrane structure, as highlighted in Section 3.2.2 for SLHF. The easiest way to tailor the overall porosity of the membrane is to choose the most adequate polymer concentration. This concept is the basis of the research study carried out by Zhao et al. [169]. A low PVDF concentration (10 - 13 wt%) was used for the outer layer to favour the formation of a sponge like-structure and highly porous selective layer whereas a higher concentration (16 - 21 wt%) in the inner solution resulted in the formation of a denser layer that provided the desired mechanical strength. In addition, using the same polymer for both the internal and external layers prevented the risk of delamination. The best performing DLHF membrane was obtained using 18 wt% of PVDF in the outer solution and 10 wt% in the inner layer. This membrane exhibited a VMD permeate flux up to 61.7 kg/m$^2$h using tap water as feed at 70°C feed temperature and a vacuum pressure of 200 mbar.

A common additive used to increase the hydrophilicity of the inner layer is polyvinyl alcohol (PVA) because of its good miscibility with PVDF [170]. The effect of PVA concentration on the DLHF membrane morphology and its MD performance was studied by Zhu et al. [160] and Feng et al. [127]. Both studies highlighted that PVA concentrations higher than 5 wt% respect to the PVDF amount could induce pore wetting but its effect can be attenuated by the spinning conditions of the outer layer. In particular, Feng et al. [127] found that using a weaker ECB (water/ethanol 50 wt%) the macrovoids formation in the outer layer was hindered and a more dense section, with slightly smaller pores, was formed.

Apart from PVA, a valuable alternative is PAN, which is a low cost polymer well miscible with PVDF [171]. This modifier was also found to effectively decrease the water contact angle of PVDF membranes and

favour the formation of large finger-like macrovoids [172]. Therefore, it was explored to increase the hydrophilicity of the inner layer of DLHF membranes [157,158,165,173]. In particular, Edwie et al. [173] prepared a hydrophilic/hydrophobic DLHF using PAN and a hydrophilic clay (Cloisite® $Na^+$) in the inner layer and compared its morphology with a hydrophobic/hydrophobic DLHF composed by two different PVDF spinning solutions and a hydrophobic clay (Cloisite® 15A). The addition of PAN effectively changed the precipitation rate of the polymer creating macrovoids in the inner layer while the hydrophobic/hydrophobic DLHF exhibited a fully globular morphology as reported in Figure 19.

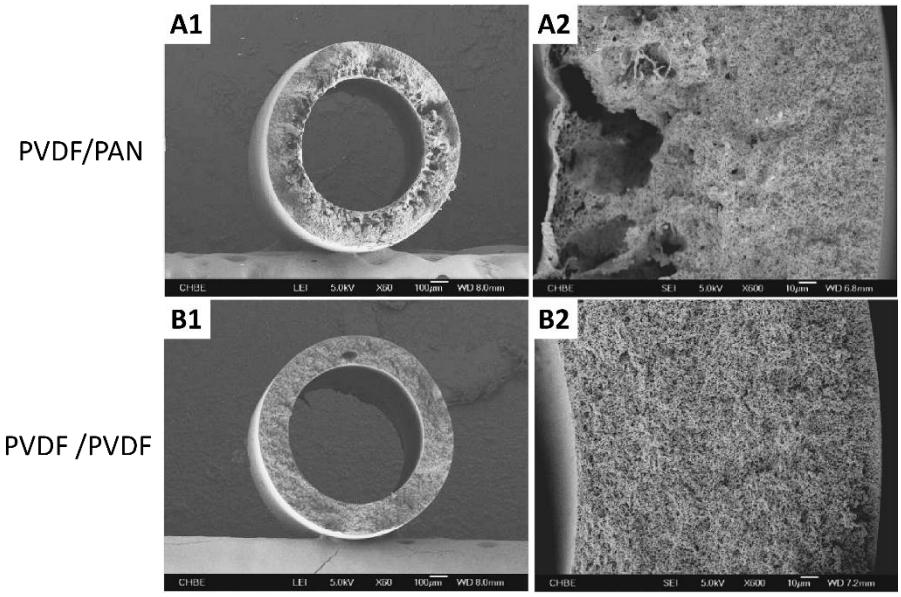


*Figure 19: Morphologies of DLHF membranes (A) DL-PVDF-PAN and (B) DL-PVDF: (1) Whole cross section, (2) High magnification cross section. Adapted from* [173].

The observed difference between the two inner layers can be attributed to the increase of the coagulation rate induced by PAN modifier. In fact, finger-like macrovoids tend to be formed at high precipitation rates related to an instantaneous liquid-liquid demixing while at low coagulation rates solid-liquid demixing becomes the main solidification path leading to an interconnected globular structure [52,174,175]. However, compared to the SLHF membrane (12 wt% PVDF, 6 wt% Cloisite® 15A), both DLHF membranes presented lower DCMD performance stability when using highly concentrated NaCl aqueous solution (24 wt%). The prepared DLHF membranes had larger pore size than that of the SLHF membrane and during long-term DCMD operations these were affected by pore wetting.

Other possible modifiers considered to change the inner layer morphology are ethylene glycol (EG) and propylene glycol (PG) [169,176]. Being miscible with water, both act as pore forming agents [177]. In particular, Bahrami et al. [178], verified that the addition of EG in the inner spinning solution improved the DCMD performance of the DLHF membrane, reaching permeate fluxes up to 38.6 kg/$m^2$h when treating 3.5 wt% NaCl aqueous solution at 80°C with 20°C permeate temperature. During a long MD operation test (100 h) these DLHF membranes also showed a good performance stability, with a low decrease in the permeate flux and the salt rejection factor.

### *5.2.4. Effect of coagulants strength*

Similar to SLHF, both BF and ECB strength play a major role in defining the final morphology of the two layers of DLHF membranes. The use of a weak nonsolvent reduces the precipitation rate of the polymer and favours the crystallization of the polymers. In this case, the surface roughness and the water contact angle are increased enhancing the membranes wetting resistance during MD operation[127,158].

Bonyadi et al. [157] found that a weak nonsolvent (methanol/water mixture of 80 wt%) used as both BF and ECB permits the preparation of PVDF DLHF membranes with a narrow pore size distribution and a mean pore size of 0.4 µm. The DLHF membranes were tested in desalination by DCMD using 3.5 wt% NaCl aqueous solution, 90°C feed temperature and 16°C permeate temperature, and the obtained permeate fluxes reached 55 kg/m$^2$h. However, these DLHF membranes were characterised by thick walls that resulted in low DCMD performance.

Baharami et al. [178] prepared PVDF DLHF membranes and investigated the effect of the nonsolvent strength using water/methanol mixtures (up to 80 wt%) as ECB and an NMP aqueous solutions, with concentrations varying from 0 to 30 wt%, as BF. The cross section and external surface images are reported in Figure 20. The reduction of the coagulation rate produced fibres with smaller inner and outer diameters, with larger pore size inner layer, and an outer layer with higher water contact angle (Figure 20 B1-B4). The cross section structure also changed from a double macrovoids layered structure when water was used as internal and external coagulant (Figure 20 A1), to a combination of an inner layer structure dominated by big macrovoids supporting an almost symmetric, globular outer layer when methanol was the main component of the ECB (Figure 20 A4).

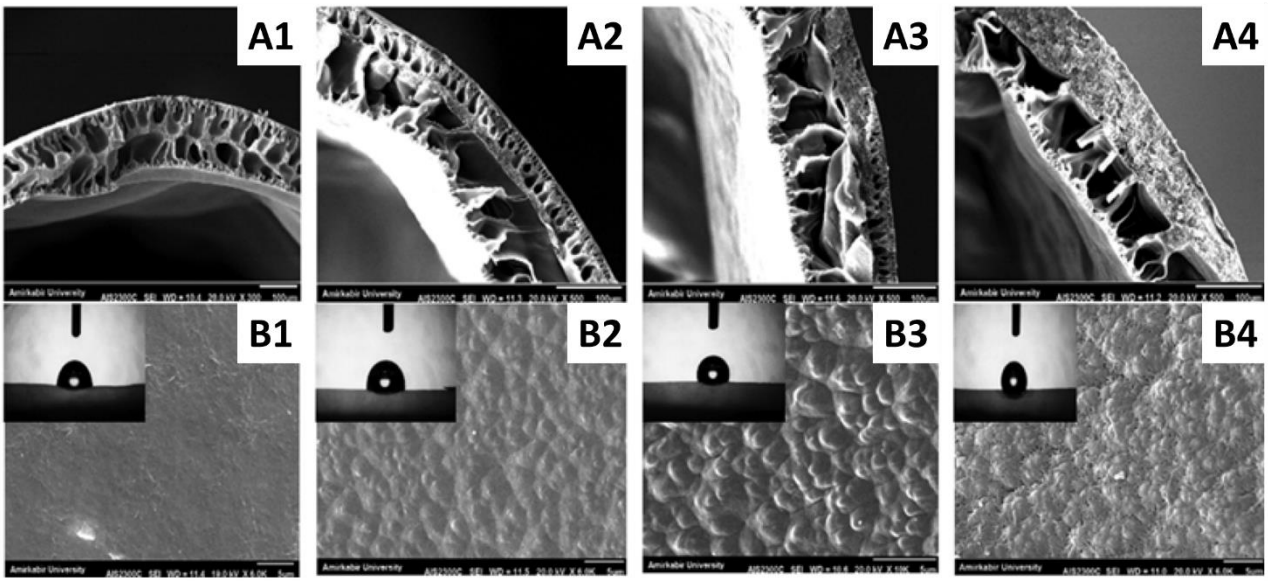


*Figure 20: Effect of different coagulation media on the hollow fibre morphology: (1) water; (2) water/methanol (60/40, w/w); (3) water/methanol (40/60, w/w) and (4) water/methanol (20/80, w/w) used as external coagulants. (A) fibre cross sections; (B) fibre external surface and contact angles. Adapted from* [178].

### *5.3. Thermal efficiency of dual layer hollow fibre membranes*

The presence of two different layers has multiple effects on the thermal efficiency of DLHF membranes. As described previously, the thermal efficiency of the process can be improved by reducing the heat loss due to heat transfer by conduction through the membrane or by increasing the permeate flux. In general, DLHF have been found to be effective in increasing the thermal efficiency of the MD process since the thinner hydrophobic layer allows to obtain higher permeate fluxes [158]. Wang et al. [168] claimed a thermal efficiency value near 94% for a highly porous structure consisting in an inner layer with large macrovoids and a thin selective outer layer. The DLHF was prepared using PVDF in both spinning solutions while PTFE particles were added in the spinning solution of the outer layer and Cloisite® 20A nano-clay was added in the spinning solution of the inner layer (Figure 18C). The large void volume caused by the finger-like macrovoids formed at the inner layer reduces the heat transfer by conduction through the membrane decreasing the thermal heat loss, while the thin hydrophobic external layer permits to obtain high permeate fluxes and a complete salt rejection. These two factors resulted in a great improvement of the overall thermal efficiency.

The importance of the membrane morphology can also be highlighted based on the results obtained by Teoh et al. [159]. It was found that the introduction of PTFE particles in the outer layer had only small effects on the thermal efficiency as both the porosity of the DLHF membranes and the permeate flux were reduced compared to the DLHF membrane prepared without filler.

### *5.4. Remarks and future directions on dual layer hollow fibre membranes*

Table 3 summarizes the main spinning conditions of DLHF membranes highlighting the effect on the membrane morphology and on the MD performance. In what follows, some remarks on the preparation and the MD performance of DLHF can be drawn.

The first problem that has to be addressed when preparing DLHF is the adhesion of the inner and outer layers avoiding any possible delamination [129]. This can be tackled by controlling the precipitation rates of both layers [153]. The delamination can be generally avoided using the same polymer for both the inner and outer spinning solutions. However, this approach prevents the optimization of the hydrophilicity of the two different layers. By tuning the two spinning compositions and the coagulation media it could be possible to obtain similar shrinking ratios for both layers even when using different polymers.

When using the same polymer for the two layers the hydrophobic/hydrophilic character of the two layers is usually tailored by adding some fillers. Similar to nanocomposite materials, the particles dispersion is a key factor defining the properties of the membrane. The development of well compatibilized nanoparticles with the polymeric spinning solution can improve the effectiveness of the filler enhancing the MD performance of the HF membrane.

The effects of the DLHF spinning conditions on the MD thermal efficiency haven not been deeply investigated yet and a clearer knowledge on this topic could shed light on the development of highly efficient DLHF membranes.

One of the greatest advantages of DLHF compared to SLHF is the possibility to tailor the HF with a thin hydrophobic layer acting as a selective part of the DLHF, while a thicker support provides the needed mechanical properties. Since the mass transfer resistance is proportional to the membrane thickness and this resistance is predominant in the selective layer, the permeate flux can be greatly enhanced by reducing the hydrophobic skin thickness. For instance, hydrophobic layers as thin as 6 μm were achieved [159].

Future research on DLHF membrane engineering should focus on the development of thin and highly porous hydrophobic layers by means of fillers such as nano-additives and adequate spinning conditions to improve their hydrophobic character keeping high its selectivity. On the other hand, the supporting layer must be prepared with very high hydrophilicity and porosity maintaining the needed mechanical properties and avoiding any possible delamination. Again, the use of inorganic nano-fillers seems promising since it is theoretically possible to improve all these factors by selecting a proper filler and an adequate concentration in the spinning solution.

The majority of the developed research studies considered a single filler for each layer. Mixed fillers with different geometries and chemical composition in the same spinning solution should be explored in order to tune HF membranes with different properties suitable for MD desalination.

*Table 3: Spinning conditions and MD performance of dual layer hollow fibre membranes.*

| Ref. | Inner Dope Composition (wt%) | Outer Dope Composition (wt%) | BF (wt%) | ECB (wt%) | Inner Thickness (μm) | Outer Thickness (μm) | Pore Size (μm) | Porosity (%) | MD test Conditions | Permeate flux (kg/m²h) |
|---|---|---|---|---|---|---|---|---|---|---|
| Khayet et al. [50] | PEI/NMP/ γ-BL /FPA (14/74/10/2) | | $H_2O$ | $H_2O$ | - | - | Out 0.08 | 65.5 | DCMD 30g/L NaCl $T_f$ = 80°C $T_p$ = 20°C | 23.8 |
| | PEI/NMP/ γ-BL /FPA (15/73/10/2) | | | | | | Out 0.08 | 54.4 | | 9.5 |
| | PEI/NMP/ γ-BL /FPA (17/71/10/2) | | | | | | Out 0.08 | 44.9 | | 1.9 |
| Feng et al. [127] | PVDF/NMP/PVA (14.2/85/0.8) | PVDF/NMP (12/88) | MeOH/$H_2O$ (80/20) | EtOH/$H_2O$ (50/50) | 103 | 17 | 0.02 | 61.1 | DCMD 3% NaCl $T_f$ = 65°C $T_p$ = 17°C | 7.8 |
| | PVDF/NMP/PVA (12/85/3) | | | | 107 | 18 | 0.02 | 78.2 | | 8.5 |
| Zuo et al. [155] | Ultem®/NMP (12.5/ 87.5) | PVDF/NMP (10/90) | NMP/$H_2O$ (50/50) | IPA/$H_2O$ (50/50) | | | | - | VMD 3.5% NaCl $T_f$ = 60°C $P_v$ = 20 mbar | 2.4 |
| | Ultem®/NMP/$Al_2O_3$ (12.5/82.5/5) | | | | | | | | | 6.0 |
| | Ultem®/NMP/$Al_2O_3$ (12.5/77.5/10) | | | | | | | | | 15.3 |
| | Ultem®/NMP/$Al_2O_3$ (12.5/72.5/15) | | | | | | | | | 27.9 |
| Bonyadi et al. [157] | PVDF/NMP/PAN/Cloisite $Na^+$ (8.24/82.35/3.53/5.88) | PVDF/NMP/Cloisite 15A (12.1/84.3/3.6) | MeOH/$H_2O$ (80/20) | MeOH/$H_2O$ (80/20) | 330 | 50 | 0.41 | 80 | DCMD 3.5% NaCl $T_f$ = 90°C $T_p$ = 16°C | 55.2 |
| Edwie et al. [158] | PVDF/NMP/PAN/Cloisite $NA^+$/EG (10/75/4/4/7) | PVDF/NMP (12/88) | NMP/$H_2O$ (60/40) | MeOH/$H_2O$ (80/20) | 123 | 27 | Max 0.48 | 78.4 | DCMD 3.5% NaCl $T_f$ = 80°C $T_p$ = 17°C | 74.9 |
| | | PVDF/NMP/MeOH (12/78/10) | | | 90 | 29 | Max 0.47 | 75.4 | | 83.4 |
| | | PVDF/NMP/FSi/MeOH (12/73/5/10) | | | 77 | 30 | Max 0.35 | 69.5 | | 77.0 |
| Teoh et al. [159] | PVDF/NMP/EG (15/70/15) | PVDF/NMP/EG/PTFE (14,6/68,0/14,6/2,9) | NMP/$H_2O$ (85/15) | IPA/$H_2O$ (60/40) | 134 | 6 | Max 0.26 | 85.5 | DCMD 3.5% NaCl $T_f$ = 80°C $T_p$ = 17°C | 56.4 |
| | | PVDF/NMP/EG/PTFE (14,4/67,0/14,4/4,3) | | | 132 | 13 | Max 0.26 | 82.5 | | 51.0 |

| | | | | | | | | | | |
|---|---|---|---|---|---|---|---|---|---|---|
| | | PVDF/NMP/EG/PTFE (14,2/66,0/14,2/5,7) | | | 130 | 20 | Max 0.26 | 81.9 | | 48.7 |
| Zhu et al. [160] | PVDF/NMP/PVA (14.2/85/0.8) | PVDF/NMP/PVP (12/78/10) | MeOH/$H_2O$ (80/20) | MeOH/$H_2O$ (80/20) | 255 | 47 | 0.02 | - | DCMD 3% NaCl $T_f$ = 65°C $T_p$ = 17°C | 7.6 |
| | | PVDF/NMP/Glycerol (12/78/10) | | | 170 | 53 | 0.02 | | | 6.0 |
| Su et al. [165] | PVDF/NMP/PAN/Cloisite $Na^+$/Graphite (9.2/69/3.9/4.9/13) | PVDF/NMP/Cloisite 15A (12.1/84.3/3.6) | $H_2O$ | MeOH/$H_2O$ (80/20) | 227 | 50 | 0.41 Theor. | 67 | DCMD 3.5% NaCl $T_f$ = 80°C $T_p$ =15°C | 41.1 |
| | PVDF/NMP/PAN/Cloisite $Na^+$/Graphite/MWNT (7.4/71.8/3.2/4.4/11.7/1.5) | | | | 232 | 50 | 0.41 Theor. | 55 | | 45.5 |
| | PVDF/NMP/PAN/Cloisite $Na^+$/Graphite/MWNT (6.1/73.5/2.6/4.1/10.8/2.9) | | | | 221 | 50 | 0.41 Theor. | 70 | | 66.9 |
| Wang et al. [168] | PVDF/NMP/EG/Cloisite 20A (10/77/10/3) | PVDF/NMP/EG/PTFE (12/77/8/3) | $H_2O$ | IPA/$H_2O$ (60/40) | 102 | 39 | | 84.0 | DCMD 3.5% NaCl $T_f$ = 80°C $T_p$ = 17°C | 98.6 |
| Zhao et al. [169] | PVDF/DMAc/PG (18/60/22) | PVDF/DMAc/PG (10/68/22) | $H_2O$ | $H_2O$ | | | 0.35 | - | VMD $H_2O$ $T_f$ = 70°C $P_v$ = 20 mbar | 61.8 |
| | PVDF/DMAc/PG (20/58/22) | | | | | | 0.32 | | | 50.1 |
| Edwie et al. [173] | PVDF/NMP/PAN/Cloisite $NA^+$/EG (10/75/4/4/7) | PVDF /NMP/MeOH 12/78/10 | NMP/$H_2O$ (60/40) | MeOH/$H_2O$ (50/50) | 142 | 60 | Max 0.26 | 83.4 | DCMD 24% NaCl $T_f$ = 60°C $T_p$ = 17°C | 13.3 |
| | PVDF/NMP/Cloisite 15A/EG (12/75/6/7) | | | | 170 | | Max 0.26 | 78.1 | | 8.5 |
| Bahrami et al. [178] | PVDF/NMP (7.1/92.9) | PVDF/NMP (13.5/86.5) | $H_2O$ | $H_2O$ | 88 | 51 | 0.5 | 75.2 | DCMD 3.5% NaCl $T_f$ = 80°C $T_p$ = 20°C | 23.8 |
| | PVDF/NMP/EG (7.1/86.9/6) | | NMP/$H_2O$ (20/80) | MeOH/$H_2O$ (60/40) | 77 | 54 | 0.4 | 87.3 | | 38.4 |

EtOH: ethanol

MeOH: methanol

## 6. Comparison of different HF morphological structures

Table 4 shows the characteristics and the MD desalination performance of the best HF membranes reported so far on single layer, dual layer and mixed matrix hollow fibre membranes together with their important spinning parameters. This selection is based on the great improvement of the permeate flux without sacrificing the salt rejection factor reported for MD operation carried out under similar conditions (DCMD, feed: 3.5 wt% NaCl solution, $T_f \approx 80°C$, $T_p \approx 17°C$). This table is useful since it permits to understand the advantages and improvements of HF membrane preparation adopting different morphological structures for desalination by MD. The comparison of these three membranes is reasonable since the design of MMHF and DLHF membranes were based on the spinning solution employed for SLHF membrane preparation. In addition, the MD operating conditions are similar. These HF membranes with different morphological structures shows a natural evolution of the research on this topic: first, a competitive SLHF was prepared [53]; then, based on the spinning solution of the SLHF membrane, additives were considered to prepare MMHF membrane [104]; and finally, this mixed matrix spinning solution was employed for the preparation of the inner layer of the DLHF membrane while a similar dope solution (with a different additive) was used for the external layer [168]. All spinning parameters were adjusted and changed to prepare suitable MD HF membranes with different morphological structures.

*Table 4: Characteristics and performance of the best single layer, mixed matrix and dual layer hollow fibre membranes used in desalination by MD under similar operating conditions.*

| Ref. | Type | Dope solution composition (wt%) | | Thickness (μm) | | Porosity (%) | MD conditions | Permeate flux (kg/m²h) |
|---|---|---|---|---|---|---|---|---|
| Wang et al. [53] | SLHF | PVDF/NMP/EG (12/80/8) | | 110 | | 73.8 | DCMD 3.5% NaCl $T_f$ = 80°C $T_p$ = 17.5°C | 41.5 |
| Wang et al. [104] | MMHF | PVDF/NMP/EG/Cloisite 20A (10.0/74.7/12.0/3.3) | | 180 | | 86.7 | DCMD 3.5% NaCl $T_f$ = 81.5°C $T_p$ = 17.5°C | 79.2 |
| Wang et al. [168] | DLHF | Inner layer (I.L.): PVDF/NMP/EG/Cloisite 20A (10/77/10/3) | Outer layer (O.L.): PVDF/NMP/EG/PTFE (12/77/8/3) | I.L. 102 | O.L. 39 | 84.0 | DCMD 3.5% NaCl $T_f$ = 80°C $T_p$ = 17°C | 98.6 |

The comparison between the best SLHF, MMHF and DLHF reported in Table 4 shows the important improvements that can be achieved when exploring different HF types. The selected SLHF [53] was prepared adding a weak nonsolvent (EG) into the PVDF/NMP spinning solution. In this way, the precipitation rate of the polymer was slowed and a rougher outer surface was obtained with an improved hydrophobic character compared with the HF prepared without EG in the spinning solution. Moreover, the addition of this

nonsolvent increased the porosity of the HF membranes resulting in a great increase of the DCMD flux (from 9 kg/m$^2$h to 41.5 kg/m$^2$h).

Several works analysed in Section 4 highlighted that the concentration of the filler plays a key role in defining the HF performance. In this regard, mixed matrix HF membranes offer competitive DCMD desalination performance. Among the various researches discussed previously, Wang et al. [104] were able to obtain the highest DCMD flux incorporating Cloisite® 20A nanoclay as filler (79.2 kg/m$^2$h) even greater than that of SLHF under the same DCMD operation conditions.

A further optimization of HF performance can be obtained preparing DLHF. The use of a second dope solution to build a selective layer supported on a highly porous hydrophilic layer that provides the needed mechanical properties, allows to reduce the mass transfer resistance by decreasing the thickness of the hydrophobic layer and result in a tremendous enhancement of the DCMD permeate flux (up to 98.6 kg/m$^2$h) without sacrificing the salt rejection factor [168]. This achieved permeate flux is almost 2.4 that of SLHF carried out under the same DCMD operation conditions.

## 7. Conclusions and future trends

Robust MD membranes can be prepared by NIPS or TIPS techniques as hollow fibres with different morphological structures such as single layer hollow fibre, mixed matrix hollow fibre or dual layered hydrophobic/hydrophilic hollow fibre. This last type of hollow fibres should exhibit thin hydrophobic layer with small pores supported by a thicker hydrophilic layer with bigger pores.

In general, to prepare single layer HF, the choice of TIPS or NIPS technique is important to tailor different morphologies. TIPS procedure commonly results in a membrane with more symmetric structure without macrovoids, while NIPS procedure results in a membrane cross section with a thin selective layer supported by a layer with finger-like structure. The choice of the spinning solution composition is a key parameter for both techniques and factors like the polymer concentration and the polymer-solvent-nonsolvent interactions can deeply change the coagulation path and the HF membrane characteristics. Spinning SLHF requires obeying some compromises. For instance, the HF membrane wall must impart the necessary mechanical resistance to withstand the MD operation conditions and therefore the thickness cannot be reduced under a certain limit. On the other hand, thicker HF result in a higher mass transfer resistance and lower permeate fluxes.

An effective and simple way to improve HF performance is the addition of different types of fillers including nano-additives to prepare mixed matrix HF. Their addition was found to have great impact on the HF membrane porosity and permeability as well as on their mechanical properties, but systematic studies are still required using high filler(s) loadings in the polymer matrix avoiding the defects associated to the agglomeration of filler(s) and reduction of the MD permeate flux, and increasing their long-term MD operation.

Some efforts have been focused on the preparation of dual layer HF membranes. Using two different polymers, with different hydrophobic character, allows to optimize both the selective and the support layer properties. However, delamination of the two layers is a common issue when this approach is followed. More attempts are still needed to improve the adhesion of the two layers in order to obtain delamination free DLHF.

The preparation of DLHF using different spinning solutions but with the same polymer was another alternative. This has been widely studied for PVDF using different additives such as nanoclays and alumina to impart the necessary hydrophilic character to one of the two layers. The internal and external coagulants were found to highly influence the structures of the layers. In particular, the use of weak nonsolvents hinders the formation of dense layers, creates a more porous structure and results in higher permeate fluxes. DLHF is formed by two layers of different hydrophobic characters. The most hydrophobic layer must be in contact with the feed solution while the most hydrophilic one must be brought into contact with the permeate side. The hydrophobicity of the feed/membrane layer of DLHF membranes could be improved using different fillers such as carbon nanotubes or hydrophobic nanoparticles. In this way, selective skin layers with high porosity and low thickness could provide the needed resistance to pore wetting and a low mass transfer resistance. At the same time, the mechanical properties of the support layer must be improved in order to withstand the MD operating conditions avoiding the HF collapse or rupture.

The effects of various involved HF spinning parameters and polymer solutions have been investigated. A deep and systematic studies on the effects of all the aforementioned parameters deserves further efforts in order to improve the MD performance of DLHF.

In order to optimize the thermal efficiency of the MD process, the heat transfer by conduction through the membrane matrix must be reduced as much as possible maintaining high the permeate flux. The best way is to increase the void volume fraction of the membrane and use materials with low thermal conductivity coefficients through the improvement of either the mixed matrix HF membranes or the dual/triple layered HF membranes. For mixed matrix HF membranes, the use of fillers with high thermal conductivity coefficients (e.g. carbon nanotubes) can reduce the thermal efficiency of the MD process. However, this effect can be alleviated by the enhancement of the permeate flux that increased the heat transfer associated to mass transfer respect to the heat loss by conduction through the membrane. DLHF membranes have been found to be effective in increasing the thermal efficiency of the MD process since the thinner hydrophobic layer allows to obtain high permeate fluxes while the thicker hydrophilic layer reduces the heat transfer by conduction following Fourier's law.

we do believe that a lot of efforts should be devoted to the improvement of HF membranes in order to boost MD toward large scale applications because of their outstanding characteristics compared to flat-sheet membranes.

## Acknowledgments

We appreciate the financial support from the Spanish Ministry of Economy and Competitiveness through its project CTM2015-65348-C2-2-R and the Spanish Ministry of Science, Innovation and Universities through its project RTI2018-096042-B-C22. Loreto García-Fernández is thankful to Comunidad de Madrid for the financial support of the postdoctoral researcher contract "Atracción de Talento Investigador (2019-T2/AMB-15912)".

## List of abbreviations

| | |
|---|---|
| AC | Activated carbon |
| AG | Air gap |
| AGMD | Air gap membrane distillation |
| AlFu MOF | Aluminium fumarate metal-organic-framework |
| BF | Bore fluid |
| CNT | Carbon nanotube |
| DBP | Dibutyl phthalate |
| DCMD | Direct contact membrane distillation |
| DEP | Diethyl phthalate |
| DLHF | Dual layer hollow fibre |
| DMAc | Dimethylacetamide |
| DMF | Dimethylformamide |
| DMP | Dimethyl phthalate |
| DOP | Dioctyl phthalate |
| EDX | X-ray energy dispersive |
| ECB | External coagulation bath |
| ECTFE | Ethylene chlorotrifluoroethylene copolymer |
| EG | Ethylene glycol |
| EtOH | Ethanol |
| FPA | Fluorinated polyurethane additives |
| GO | Graphene oxide |
| GTA | Glycerol triacetate |
| HDPE | High density polyethylene |
| HF | Hollow fibre |
| IPA | Isopropyl alcohol |
| LEP | Liquid entry pressure |
| LGMD | Liquid gap membrane distillation |
| MD | Membrane distillation |
| MeOH | Methanol |
| MGMD | Material gap membrane distillation |
| MMHF | Mixed matrix hollow fibres |
| MOF | Metal-organic-framework |
| MWNT | Multi wall carbon nanotube |
| NIPS | Nonsolvent induced phase separation |

| | |
|---|---|
| NMP | N-Methyl-2-pyrrolidone |
| PAN | Polyacrylonitrile |
| PC | Propylene carbonate |
| PDMS | Polydimethylsiloxane |
| PEG | Polyethylene glycol |
| PEI | Polyetherimide |
| PES | Polyethersulfone |
| PG | Propylene glycol |
| PP | Polypropylene |
| PSf | Polysulfone |
| PTFE | Polytetrafluoroethylene |
| PVA | Polyvinyl alcohol |
| PVDF | Polyvinylidene fluoride |
| PVDF-HFP | Poly(vinylidene fluoride-co-hexafluoropropylene) |
| PVP | Polyvinyl pyrrolidone |
| QB | Quenching bath |
| RO | Reverse osmosis |
| SGMD | Sweeping gas membrane distillation |
| SLHF | Single layer hollow fibre |
| TEOS | Tetraethoxysilane |
| TEP | Triethyl phosphate |
| $T_f$ | Feed temperature |
| THF | Tetrahydrofuran |
| TIPS | Thermally induced phase separation |
| TMP | Trimethyl phosphate |
| $T_p$ | Permeate temperature |
| TSGMD | Thermostatic sweeping gap membrane distillation |
| VMD | Vacuum membrane distillation |
| XPS | X-ray photoelectron spectroscopy |
| γ-BL | γ-Butyrolactone |

## References


[1] J. Glater, The early history of reverse osmosis membrane development, Desalination. 117 (1998) 297–309. doi:10.1016/S0011-9164(98)00122-2.

[2] S. Loeb, S. Sourirajan, Sea Water Demineralization by Means of an Osmotic Membrane, in: Adv. Chem. ACS, 1963: pp. 117–132. doi:10.1021/ba-1963-0038.ch009.

[3] K. Park, J. Kim, D.R. Yang, S. Hong, Towards a low-energy seawater reverse osmosis desalination plant: A review and theoretical analysis for future directions, J. Memb. Sci. 595 (2020) 117607. doi:10.1016/j.memsci.2019.117607.

[4] U. Caldera, C. Breyer, Learning Curve for Seawater Reverse Osmosis Desalination Plants: Capital Cost Trend of the Past, Present, and Future, Water Resour. Res. 53 (2017) 10523–10538.

doi:10.1002/2017WR021402.

[5] E. Drioli, A. Ali, F. Macedonio, Membrane distillation: Recent developments and perspectives, Desalination. 356 (2015) 56–84. doi:10.1016/j.desal.2014.10.028.

[6] M. Khayet, Membranes and theoretical modeling of membrane distillation: A review, Adv. Colloid Interface Sci. 164 (2011) 56–88. doi:10.1016/j.cis.2010.09.005.

[7] M.S.S. El-Bourawi, Z. Ding, R. Ma, M. Khayet, A framework for better understanding membrane distillation separation process, Elsevier, 2006. doi:10.1016/j.memsci.2006.08.002.

[8] K.W. Lawson, D.R. Lloyd, Membrane distillation, J. Memb. Sci. 124 (1997) 1–25. doi:10.1016/S0376-7388(96)00236-0.

[9] D. González, J. Amigo, F. Suárez, Membrane distillation: Perspectives for sustainable and improved desalination, Renew. Sustain. Energy Rev. 80 (2017) 238–259. doi:10.1016/j.rser.2017.05.078.

[10] J.H. Tsai, F. Macedonio, E. Drioli, L. Giorno, C.Y. Chou, F.C. Hu, C.L. Li, C.J. Chuang, K.L. Tung, Membrane-based zero liquid discharge: Myth or reality?, J. Taiwan Inst. Chem. Eng. 80 (2017) 192–202. doi:10.1016/j.jtice.2017.06.050.

[11] L. Eykens, K. De Sitter, C. Dotremont, L. Pinoy, B. Van Der Bruggen, How to Optimize the Membrane Properties for Membrane Distillation: A Review, Ind. Eng. Chem. Res. 55 (2016) 9333–9343. doi:10.1021/acs.iecr.6b02226.

[12] A. Alkhudhiri, N. Darwish, N. Hilal, Membrane distillation: A comprehensive review, Desalination. 287 (2012) 2–18. doi:10.1016/j.desal.2011.08.027.

[13] L. Eykens, K. De Sitter, C. Dotremont, L. Pinoy, B. Van der Bruggen, Membrane synthesis for membrane distillation: A review, Sep. Purif. Technol. 182 (2017) 36–51. doi:10.1016/j.seppur.2017.03.035.

[14] M. Pagliero, A. Comite, O. Soda, C. Costa, Effect of support on PVDF membranes for distillation process, J. Memb. Sci. 635 (2021) 119528. doi:10.1016/j.memsci.2021.119528.

[15] C.F. Wan, T. Yang, G.G. Lipscomb, D.J. Stookey, T.S. Chung, Design and fabrication of hollow fiber membrane modules, J. Memb. Sci. 538 (2017) 96–107. doi:10.1016/j.memsci.2017.05.047.

[16] X. Yang, R. Wang, A.G. Fane, Novel designs for improving the performance of hollow fiber membrane distillation modules, J. Memb. Sci. 384 (2011) 52–62. doi:10.1016/j.memsci.2011.09.007.

[17] A.A. Kiss, O.M. Kattan Readi, An industrial perspective on membrane distillation processes, J. Chem. Technol. Biotechnol. 93 (2018) 2047–2055. doi:10.1002/jctb.5674.

[18] G. Zaragoza, J.A. Andrés-Mañas, A. Ruiz-Aguirre, Commercial scale membrane distillation for solar desalination, Npj Clean Water. 1 (2018) 20. doi:10.1038/s41545-018-0020-z.

[19] L.D. Tijing, Y.C. Woo, J.-S. Choi, S. Lee, S.-H. Kim, H.K. Shon, Fouling and its control in membrane distillation—A review, J. Memb. Sci. 475 (2015) 215–244. doi:10.1016/J.MEMSCI.2014.09.042.

[20] Y. Li, C. Jin, Y. Peng, Q. An, Z. Chen, J. Zhang, L. Ge, S. Wang, Fabrication of PVDF hollow fiber membranes via integrated phase separation for membrane distillation, J. Taiwan Inst. Chem. Eng. 95

(2019) 487–494. doi:10.1016/j.jtice.2018.08.036.

[21] M. Pagliero, A. Bottino, A. Comite, C. Costa, Novel hydrophobic PVDF membranes prepared by nonsolvent induced phase separation for membrane distillation, J. Memb. Sci. 596 (2020) 117575. doi:10.1016/j.memsci.2019.117575.

[22] Y. Su, C. Chen, Y. Li, J. Li, PVDF membrane formation via thermally induced phase separation, J. Macromol. Sci. Part A Pure Appl. Chem. 44 (2007) 99–104. doi:10.1080/10601320601044575.

[23] A. Figoli, Thermally Induced Phase Separation (TIPS) for Membrane Preparation, in: Encycl. Membr., Springer Berlin Heidelberg, Berlin, Heidelberg, 2014: pp. 1–2. doi:10.1007/978-3-642-40872-4_1866-1.

[24] A.G. Fane, C.Y. Tang, R. Wang, Membrane Technology for Water: Microfiltration, Ultrafiltration, Nanofiltration, and Reverse Osmosis, Treatise Water Sci. 4 (2011) 301–335. doi:10.1016/B978-0-444-53199-5.00091-9.

[25] M. Khayet, T. Matsuura, Membrane Distillation: Principles and Applications, Elsevier, 2011. doi:10.1016/C2009-0-17487-1.

[26] K.Y. Wang, T. Matsuura, T.S. Chung, W.F. Guo, The effects of flow angle and shear rate within the spinneret on the separation performance of poly(ethersulfone) (PES) ultrafiltration hollow fiber membranes, J. Memb. Sci. 240 (2004) 67–79. doi:10.1016/j.memsci.2004.04.012.

[27] A.F. Ismail, S.J. Shilton, I.R. Dunkin, S.L. Gallivan, Direct measurement of rheologically induced molecular orientation in gas separation hollow fibre membranes and effects on selectivity, J. Memb. Sci. 126 (1997) 133–137. doi:10.1016/S0376-7388(96)00274-8.

[28] W. Nijdam, J. De Jong, C.J.M. Van Rijn, T. Visser, L. Versteeg, G. Kapantaidakis, G.H. Koops, M. Wessling, High performance micro-engineered hollow fiber membranes by smart spinneret design, J. Memb. Sci. 256 (2005) 209–215. doi:10.1016/j.memsci.2005.02.022.

[29] P.Z. Çulfaz, E. Rolevink, C. van Rijn, R.G.H. Lammertink, M. Wessling, Microstructured hollow fibers for ultrafiltration, J. Memb. Sci. 347 (2010) 32–41. doi:10.1016/j.memsci.2009.10.003.

[30] L. García-Fernández, C. García-Payo, M. Khayet, Hollow fiber membranes with different external corrugated surfaces for desalination by membrane distillation, Appl. Surf. Sci. 416 (2017) 932–946. doi:10.1016/j.apsusc.2017.04.232.

[31] X. Yang, H. Yu, R. Wang, A.G. Fane, Optimization of microstructured hollow fiber design for membrane distillation applications using CFD modeling, J. Memb. Sci. 421–422 (2012) 258–270. doi:10.1016/j.memsci.2012.07.022.

[32] T. Luelf, D. Rall, D. Wypysek, M. Wiese, T. Femmer, C. Bremer, J.U. Michaelis, M. Wessling, 3D-printed rotating spinnerets create membranes with a twist, J. Memb. Sci. 555 (2018) 7–19. doi:10.1016/j.memsci.2018.03.026.

[33] T. Luelf, M. Tepper, H. Breisig, M. Wessling, Sinusoidal shaped hollow fibers for enhanced mass

transfer, J. Memb. Sci. 533 (2017) 302–308. doi:10.1016/j.memsci.2017.03.030.

[34] H. Roth, M. Alders, T. Luelf, S. Emonds, S.I. Mueller, M. Tepper, M. Wessling, Chemistry in a spinneret — Sinusoidal-shaped composite hollow fiber membranes, J. Memb. Sci. 585 (2019) 115–125. doi:10.1016/j.memsci.2019.05.029.

[35] L. García-Fernández, M.C. García-Payo, M. Khayet, Mechanism of formation of hollow fiber membranes for membrane distillation: 2. Outer coagulation power effect on morphological characteristics, J. Memb. Sci. 542 (2017) 469–481. doi:10.1016/j.memsci.2017.03.038.

[36] Z. Cui, N.T. Hassankiadeh, S.Y. Lee, J.M. Lee, K.T. Woo, A. Sanguineti, V. Arcella, Y.M. Lee, E. Drioli, Poly(vinylidene fluoride) membrane preparation with an environmental diluent via thermally induced phase separation, J. Memb. Sci. 444 (2013) 223–236. doi:10.1016/j.memsci.2013.05.031.

[37] Y. Tang, N. Li, A. Liu, S. Ding, C. Yi, H. Liu, Effect of spinning conditions on the structure and performance of hydrophobic PVDF hollow fiber membranes for membrane distillation, Desalination. 287 (2012) 326–339. doi:10.1016/j.desal.2011.11.045.

[38] M. Khayet, The effects of air gap length on the internal and external morphology of hollow fiber membranes, Chem. Eng. Sci. 58 (2003) 3091–3104. doi:10.1016/S0009-2509(03)00186-6.

[39] D. Wang, K. Li, W.. Teo, Preparation and characterization of polyvinylidene fluoride (PVDF) hollow fiber membranes, J. Memb. Sci. 163 (1999) 211–220. doi:10.1016/S0376-7388(99)00181-7.

[40] M. Khayet, M.C. García-Payo, F.A. Qusay, K.C. Khulbe, C.Y. Feng, T. Matsuura, Effects of gas gap type on structural morphology and performance of hollow fibers, J. Memb. Sci. 311 (2008) 259–269. doi:10.1016/j.memsci.2007.12.041.

[41] M. Khayet, M.C. García-Payo, X-Ray diffraction study of polyethersulfone polymer, flat-sheet and hollow fibers prepared from the same under different gas-gaps, Desalination. 245 (2009) 494–500. doi:10.1016/j.desal.2009.02.013.

[42] Y.R. Qiu, N.A. Rahman, H. Matsuyama, Preparation of hydrophilic poly(vinyl butyral)/Pluronic F127 blend hollow fiber membrane via thermally induced phase separation, Sep. Purif. Technol. 61 (2008) 1–8. doi:10.1016/j.seppur.2007.09.014.

[43] H. Matsuyama, H. Okafuji, T. Maki, M. Teramoto, N. Kubota, Preparation of polyethylene hollow fiber membrane via thermally induced phase separation, J. Memb. Sci. 223 (2003) 119–126. doi:10.1016/S0376-7388(03)00314-4.

[44] N.T. Hassankiadeh, Z. Cui, J.H. Kim, D.W. Shin, A. Sanguineti, V. Arcella, Y.M. Lee, E. Drioli, PVDF hollow fiber membranes prepared from green diluent via thermally induced phase separation: Effect of PVDF molecular weight, J. Memb. Sci. 471 (2014) 237–246. doi:10.1016/j.memsci.2014.07.060.

[45] H. Karkhanechi, S. Rajabzadeh, E. Di Nicolò, H. Usuda, A.R. Shaikh, H. Matsuyama, Preparation and characterization of ECTFE hollow fiber membranes via thermally induced phase separation (TIPS), Polymer (Guildf). 97 (2016) 515–524. doi:10.1016/j.polymer.2016.05.067.

[46] B. Wu, K. Li, W.K. Teo, Preparation and characterization of poly(vinylidene fluoride) hollow fiber membranes for vacuum membrane distillation, J. Appl. Polym. Sci. 106 (2007) 1482–1495. doi:10.1002/app.26624.

[47] R. Naim, A.F. Ismail, A. Mansourizadeh, Effect of non-solvent additives on the structure and performance of PVDF hollow fiber membrane contactor for CO 2 stripping, J. Memb. Sci. 423–424 (2012) 503–513. doi:10.1016/j.memsci.2012.08.052.

[48] A. Bottino, G. Capannelli, S. Munari, A. Turturro, High performance ultrafiltration membranes cast from LiCl doped solutions, Desalination. 68 (1988) 167–177. doi:10.1016/0011-9164(88)80052-3.

[49] F. Liu, N.A. Hashim, Y. Liu, M.R.M. Abed, K. Li, Progress in the production and modification of PVDF membranes, J. Memb. Sci. 375 (2011) 1–27. doi:10.1016/j.memsci.2011.03.014.

[50] M. Khayet, M. Essalhi, M.R. Qtaishat, T. Matsuura, Robust surface modified polyetherimide hollow fiber membrane for long-term desalination by membrane distillation, Desalination. 466 (2019) 107–117. doi:10.1016/j.desal.2019.05.008.

[51] M.C. García-Payo, M. Essalhi, M. Khayet, Effects of PVDF-HFP concentration on membrane distillation performance and structural morphology of hollow fiber membranes, J. Memb. Sci. 347 (2010) 209–219. doi:10.1016/j.memsci.2009.10.026.

[52] P. Sukitpaneenit, T.S. Chung, Molecular elucidation of morphology and mechanical properties of PVDF hollow fiber membranes from aspects of phase inversion, crystallization and rheology, J. Memb. Sci. 340 (2009) 192–205. doi:10.1016/j.memsci.2009.05.029.

[53] K.Y. Wang, T.S. Chung, M. Gryta, Hydrophobic PVDF hollow fiber membranes with narrow pore size distribution and ultra-thin skin for the fresh water production through membrane distillation, Chem. Eng. Sci. 63 (2008) 2587–2594. doi:10.1016/j.ces.2008.02.020.

[54] M. Yao, J. Ren, N. Akther, Y.C. Woo, L.D. Tijing, S.H. Kim, H.K. Shon, Improving membrane distillation performance: Morphology optimization of hollow fiber membranes with selected non-solvent in dope solution, Chemosphere. 230 (2019) 117–126. doi:10.1016/j.chemosphere.2019.05.049.

[55] P. Wu, L.Y. Jiang, B. Hu, Fabrication of novel PVDF/P(VDF-co-HFP) blend hollow fiber membranes for DCMD, J. Memb. Sci. 566 (2018) 442–454. doi:10.1016/j.memsci.2018.09.015.

[56] L. Lin, H. Geng, Y. An, P. Li, H. Chang, Preparation and properties of PVDF hollow fiber membrane for desalination using air gap membrane distillation, Desalination. 367 (2015) 145–153. doi:10.1016/j.desal.2015.04.005.

[57] B. Zhou, Q. Li, Y. Tang, Y. Lin, X. Wang, Preparation of ECTFE membranes with bicontinuous structure via TIPS method by a binary diluent, Desalin. Water Treat. 57 (2016) 17646–17657. doi:10.1080/19443994.2015.1086898.

[58] L. García-Fernández, M.C. García-Payo, M. Khayet, Effects of mixed solvents on the structural morphology and membrane distillation performance of PVDF-HFP hollow fiber membranes, J. Memb.

Sci. 468 (2014) 324–338. doi:10.1016/j.memsci.2014.06.014.

[59] J. Kong, K. Li, Preparation of PVDF hollow-fiber membranes via immersion precipitation, J. Appl. Polym. Sci. 81 (2001) 1643–1653. doi:10.1002/app.1595.

[60] D. Hou, J. Wang, D. Qu, Z. Luan, X. Ren, Fabrication and characterization of hydrophobic PVDF hollow fiber membranes for desalination through direct contact membrane distillation, Sep. Purif. Technol. 69 (2009) 78–86. doi:10.1016/j.seppur.2009.06.026.

[61] S. Simone, A. Figoli, A. Criscuoli, M.C. Carnevale, A. Rosselli, E. Drioli, Preparation of hollow fibre membranes from PVDF/PVP blends and their application in VMD, J. Memb. Sci. 364 (2010) 219–232. doi:10.1016/j.memsci.2010.08.013.

[62] D.R. Lloyd, K.E. Kinzer, H.S.S. Tseng, Microporous membrane formation via thermally induced phase separation. I. Solid-liquid phase separation, J. Memb. Sci. 52 (1990) 239–261. doi:10.1016/S0376-7388(00)85130-3.

[63] D.R. Lloyd, S.S. Kim, K.E. Kinzer, Microporous membrane formation via thermally-induced phase separation. II. Liquid—liquid phase separation, J. Memb. Sci. 64 (1991) 1–11. doi:10.1016/0376-7388(91)80073-F.

[64] H. Matsuyama, M. Teramoto, S. Kudari, Y. Kitamura, Effect of diluents on membrane formation via thermally induced phase separation, J. Appl. Polym. Sci. 82 (2001) 169–177. doi:10.1002/app.1836.

[65] Z. Song, M. Xing, J. Zhang, B. Li, S. Wang, Determination of phase diagram of a ternary PVDF/γ-BL/DOP system in TIPS process and its application in preparing hollow fiber membranes for membrane distillation, Sep. Purif. Technol. 90 (2012) 221–230. doi:10.1016/j.seppur.2012.02.043.

[66] M. Gu, J. Zhang, X. Wang, H. Tao, L. Ge, Formation of poly(vinylidene fluoride) (PVDF) membranes via thermally induced phase separation, Desalination. 192 (2006) 160–167. doi:10.1016/j.desal.2005.10.015.

[67] J. Wang, Q. He, Y. Zhao, P. Li, H. Chang, Preparation and properties of iPP hollow fiber membranes for air gap membrane distillation, Desalin. Water Treat. 57 (2016) 23546–23555. doi:10.1080/19443994.2016.1141375.

[68] L. Shi, R. Wang, Y. Cao, D.T. Liang, J.H. Tay, Effect of additives on the fabrication of poly(vinylidene fluoride-co-hexafluropropylene) (PVDF-HFP) asymmetric microporous hollow fiber membranes, J. Memb. Sci. 315 (2008) 195–204. doi:10.1016/j.memsci.2008.02.035.

[69] W.Z. Lang, J.P. Shen, Y.X. Zhang, Y.H. Yu, Y.J. Guo, C.X. Liu, Preparation and characterizations of charged poly(vinyl butyral) hollow fiber ultrafiltration membranes with perfluorosulfonic acid as additive, J. Memb. Sci. 430 (2013) 1–10. doi:10.1016/j.memsci.2012.10.039.

[70] L. García-Fernández, M.C. García-Payo, M. Khayet, Mechanism of formation of hollow fiber membranes for membrane distillation: 1. Inner coagulation power effect on morphological characteristics, J. Memb. Sci. 542 (2017) 456–468. doi:10.1016/j.memsci.2017.03.036.

[71] N.L. Le, S.P. Nunes, Ethylene glycol as bore fluid for hollow fiber membrane preparation, J. Memb. Sci. 533 (2017) 171–178. doi:10.1016/j.memsci.2017.03.045.

[72] A. Xu, A. Yang, S. Young, D. deMontigny, P. Tontiwachwuthikul, Effect of internal coagulant on effectiveness of polyvinylidene fluoride membrane for carbon dioxide separation and absorption, J. Memb. Sci. 311 (2008) 153–158. doi:10.1016/j.memsci.2007.12.008.

[73] C. Fang, W. Liu, P. Zhang, M. Yao, S. Rajabzadeh, N. Kato, H. Kyong Shon, H. Matsuyama, Controlling the inner surface pore and spherulite structures of PVDF hollow fiber membranes in thermally induced phase separation using triple-orifice spinneret for membrane distillation, Sep. Purif. Technol. 258 (2021) 117988. doi:10.1016/j.seppur.2020.117988.

[74] J. Zuo, T.S. Chung, PVDF hollow fibers with novel sandwich structure and superior wetting resistance for vacuum membrane distillation, Desalination. 417 (2017) 94–101. doi:10.1016/j.desal.2017.05.022.

[75] K. Praneeth, B. Suresh K., T. James, S. Sridhar, Design of novel ultrafiltration systems based on robust polyphenylsulfone hollow fiber membranes for treatment of contaminated surface water, Chem. Eng. J. 248 (2014) 297–306. doi:10.1016/j.cej.2014.02.087.

[76] N. Peng, N. Widjojo, P. Sukitpaneenit, M.M. Teoh, G.G. Lipscomb, T.S. Chung, J.Y. Lai, Evolution of polymeric hollow fibers as sustainable technologies: Past, present, and future, Prog. Polym. Sci. 37 (2012) 1401–1424. doi:10.1016/j.progpolymsci.2012.01.001.

[77] S.P. Deshmukh, K. Li, Effect of ethanol composition in water coagulation bath on morphology of PVDF hollow fibre membranes, J. Memb. Sci. 150 (1998) 75–85. doi:10.1016/S0376-7388(98)00196-3.

[78] Z.W. Song, L.Y. Jiang, Optimization of morphology and perf ormance of PVDF hollow fiber for direct contact membrane distillation using experimental design, Chem. Eng. Sci. 101 (2013) 130–143. doi:10.1016/j.ces.2013.06.006.

[79] K.J. Lu, J. Zuo, T.S. Chung, Tri-bore PVDF hollow fibers with a super-hydrophobic coating for membrane distillation, J. Memb. Sci. 514 (2016) 165–175. doi:10.1016/j.memsci.2016.04.058.

[80] S. Bonyadi, T.S. Chung, W.B. Krantz, Investigation of corrugation phenomenon in the inner contour of hollow fibers during the non-solvent induced phase-separation process, J. Memb. Sci. 299 (2007) 200–210. doi:10.1016/j.memsci.2007.04.045.

[81] X. Wang, L. Zhang, D. Sun, Q. An, H. Chen, Effect of coagulation bath temperature on formation mechanism of poly(vinylidene fluoride) membrane, J. Appl. Polym. Sci. 110 (2008) 1656–1663. doi:10.1002/app.28169.

[82] L.B. Zhao, M. Liu, Z.L. Xu, Y.M. Wei, M.X. Xu, PSF hollow fiber membrane fabricated from PSF-HBPE-PEG400-DMAc dope solutions via reverse thermally induced phase separation (RTIPS) process, Chem. Eng. Sci. 137 (2015) 131–139. doi:10.1016/j.ces.2015.06.017.

[83] N. Ghasem, M. Al-Marzouqi, A. Duaidar, Effect of quenching temperature on the performance of poly(vinylidene fluoride) microporous hollow fiber membranes fabricated via thermally induced

phase separation technique on the removal of CO2 from CO2-gas mixture, Int. J. Greenh. Gas Control. 5 (2011) 1550–1558. doi:10.1016/j.ijggc.2011.08.012.

[84] A. Santmartí, K.-Y. Lee, Crystallinity and Thermal Stability of Nanocellulose, in: Nanocellulose Sustain., CRC Press, Boca Raton : CRC Press, [2018] | Series: Sustainability contributions through science and technology, 2018: pp. 67–86. doi:10.1201/9781351262927-5.

[85] R. Wang, T.-S. Chung, Determination of pore sizes and surface porosity and the effect of shear stress within a spinneret on asymmetric hollow fiber membranes, J. Memb. Sci. 188 (2001) 29–37. doi:10.1016/S0376-7388(01)00370-2.

[86] J. Qin, Effect of wet and dry-jet wet spinning on the shear-induced orientation during the formation of ultrafiltration hollow fiber membranes, J. Memb. Sci. 182 (2001) 57–75. doi:10.1016/S0376-7388(00)00552-4.

[87] M. Radjabian, J. Koll, K. Buhr, U.A. Handge, V. Abetz, Hollow fiber spinning of block copolymers: Influence of spinning conditions on morphological properties, Polymer (Guildf). 54 (2013) 1803–1812. doi:10.1016/j.polymer.2013.01.033.

[88] K. Smolders, A.C.M. Franken, Terminology for Membrane Distillation, 1989.

[89] Y. Zhang, Y. Peng, S. Ji, Z. Li, P. Chen, Review of thermal efficiency and heat recycling in membrane distillation processes, Desalination. 367 (2015) 223–239. doi:10.1016/j.desal.2015.04.013.

[90] J. Zhao, L. Shi, C.H. Loh, R. Wang, Preparation of PVDF/PTFE hollow fiber membranes for direct contact membrane distillation via thermally induced phase separation method, Desalination. 430 (2018) 86–97. doi:10.1016/j.desal.2017.12.041.

[91] Y. Song, Z. Wang, Q. Wang, B. Li, B. Zhong, Preparation of PVDF/CaCO3 hybrid hollow fiber membranes for direct contact membrane distillation through TIPS method, J. Appl. Polym. Sci. 133 (2016) 1–11. doi:10.1002/app.43372.

[92] D. Qadir, H. Mukhtar, L.K. Keong, Mixed Matrix Membranes for Water Purification Applications, Sep. Purif. Rev. 46 (2017) 62–80. doi:10.1080/15422119.2016.1196460.

[93] M.A. Aroon, A.F. Ismail, T. Matsuura, M.M. Montazer-Rahmati, Performance studies of mixed matrix membranes for gas separation: A review, Sep. Purif. Technol. 75 (2010) 229–242. doi:10.1016/j.seppur.2010.08.023.

[94] A. Elrasheedy, N. Nady, M. Bassyouni, A. El-Shazly, Metal organic framework based polymer mixed matrix membranes: Review on applications in water purification, Membranes (Basel). 9 (2019) 88. doi:10.3390/membranes9070088.

[95] J. Dechnik, J. Gascon, C.J. Doonan, C. Janiak, C.J. Sumby, Mixed-Matrix Membranes, Angew. Chemie - Int. Ed. 56 (2017) 9292–9310. doi:10.1002/anie.201701109.

[96] S. Beisl, S. Monteiro, R. Santos, A.S. Figueiredo, M.G. Sánchez-Loredo, M.A. Lemos, F. Lemos, M. Minhalma, M.N. de Pinho, Synthesis and bactericide activity of nanofiltration composite membranes

– Cellulose acetate/silver nanoparticles and cellulose acetate/silver ion exchanged zeolites, Water Res. 149 (2019) 225–231. doi:10.1016/j.watres.2018.10.096.

[97] L. Dong, H. Yang, S. Liu, X. Wang, Y.F. Xie, Fabrication and anti-biofouling properties of alumina and zeolite nanoparticle embedded ultrafiltration membranes, Desalination. 365 (2015) 70–78. doi:10.1016/j.desal.2015.02.023.

[98] L. Peng, X. Xu, X. Yao, H. Liu, X. Gu, Fabrication of novel hierarchical ZSM-5 zeolite membranes with tunable mesopores for ultrafiltration, J. Memb. Sci. 549 (2018) 446–455. doi:10.1016/j.memsci.2017.12.039.

[99] H. Dong, L. Zhao, L. Zhang, H. Chen, C. Gao, W.S. Winston Ho, High-flux reverse osmosis membranes incorporated with NaY zeolite nanoparticles for brackish water desalination, J. Memb. Sci. 476 (2015) 373–383. doi:10.1016/j.memsci.2014.11.054.

[100] D. Hou, J. Wang, X. Sun, Z. Ji, Z. Luan, Preparation and properties of PVDF composite hollow fiber membranes for desalination through direct contact membrane distillation, J. Memb. Sci. 405–406 (2012) 185–200. doi:10.1016/j.memsci.2012.03.008.

[101] H. Zhang, B. Li, D. Sun, X. Miao, Y. Gu, SiO2-PDMS-PVDF hollow fiber membrane with high flux for vacuum membrane distillation, Desalination. 429 (2018) 33–43. doi:10.1016/j.desal.2017.12.004.

[102] J.A. Prince, G. Singh, D. Rana, T. Matsuura, V. Anbharasi, T.S. Shanmugasundaram, Preparation and characterization of highly hydrophobic poly(vinylidene fluoride) – Clay nanocomposite nanofiber membranes (PVDF–clay NNMs) for desalination using direct contact membrane distillation, J. Memb. Sci. 397–398 (2012) 80–86. doi:10.1016/j.memsci.2012.01.012.

[103] N.M. Mokhtar, W.J. Lau, A.F. Ismail, B.C. Ng, Physicochemical study of polyvinylidene fluoride-Cloisite15A® composite membranes for membrane distillation application, RSC Adv. 4 (2014) 63367–63379. doi:10.1039/c4ra10289d.

[104] K.Y. Wang, S.W. Foo, T.-S.S. Chung, Mixed matrix PVDF hollow fiber membranes with nanoscale pores for desalination through direct contact membrane distillation, Ind. Eng. Chem. Res. 48 (2009) 4474–4483. doi:10.1021/ie8009704.

[105] N.M. Mokhtar, W.J. Lau, A.F. Ismail, W. Youravong, W. Khongnakorn, K. Lertwittayanon, Performance evaluation of novel PVDF-Cloisite 15A hollow fiber composite membranes for treatment of effluents containing dyes and salts using membrane distillation, RSC Adv. 5 (2015) 38011–38020. doi:10.1039/c5ra00182j.

[106] N.M. Mokhtar, W.J. Lau, A.F. Ismail, S. Kartohardjono, S.O. Lai, H.C. Teoh, The potential of direct contact membrane distillation for industrial textile wastewater treatment using PVDF-Cloisite 15A nanocomposite membrane, Chem. Eng. Res. Des. 111 (2016) 284–293. doi:10.1016/j.cherd.2016.05.018.

[107] H.B. Tanh Jeazet, C. Staudt, C. Janiak, Metal–organic frameworks in mixed-matrix membranes for gas

separation, Dalt. Trans. 41 (2012) 14003. doi:10.1039/c2dt31550e.

[108] N. Stock, S. Biswas, Synthesis of Metal-Organic Frameworks (MOFs): Routes to Various MOF Topologies, Morphologies, and Composites, Chem. Rev. 112 (2012) 933–969. doi:10.1021/cr200304e.

[109] D. Cheng, L. Zhao, N. Li, S.J.D. Smith, D. Wu, J. Zhang, D. Ng, C. Wu, M.R. Martinez, M.P. Batten, Z. Xie, Aluminum fumarate MOF/PVDF hollow fiber membrane for enhancement of water flux and thermal efficiency in direct contact membrane distillation, J. Memb. Sci. 588 (2019) 117204. doi:10.1016/j.memsci.2019.117204.

[110] B.J. Cha, J.M. Yang, Effect of high-temperature spinning and PVP additive on the properties of PVDF hollow fiber membranes for microfiltration, Macromol. Res. 14 (2006) 596–602. doi:10.1007/BF03218730.

[111] C. Athanasekou, A. Sapalidis, I. Katris, E. Savopoulou, K. Beltsios, T. Tsoufis, A. Kaltzoglou, P. Falaras, G. Bounos, M. Antoniou, P. Boutikos, G.E. Romanos, Mixed Matrix PVDF/Graphene and Composite-Skin PVDF/Graphene Oxide Membranes Applied in Membrane Distillation, Polym. Eng. Sci. 59 (2019) E262–E278. doi:10.1002/pen.24930.

[112] L. Zhao, X. Lu, C. Wu, Q. Zhang, Flux enhancement in membrane distillation by incorporating AC particles into PVDF polymer matrix, J. Memb. Sci. 500 (2016) 46–54. doi:10.1016/j.memsci.2015.11.010.

[113] S. Pei, H.-M. Cheng, The reduction of graphene oxide, Carbon N. Y. 50 (2012) 3210–3228. doi:10.1016/j.carbon.2011.11.010.

[114] K.H. Chu, M. Fathizadeh, M. Yu, J.R.V. Flora, A. Jang, M. Jang, C.M. Park, S.S. Yoo, N. Her, Y. Yoon, Evaluation of Removal Mechanisms in a Graphene Oxide-Coated Ceramic Ultrafiltration Membrane for Retention of Natural Organic Matter, Pharmaceuticals, and Inorganic Salts, ACS Appl. Mater. Interfaces. 9 (2017) 40369–40377. doi:10.1021/acsami.7b14217.

[115] S. Leaper, A. Abdel-Karim, B. Faki, J.M. Luque-Alled, M. Alberto, A. Vijayaraghavan, S.M. Holmes, G. Szekely, M.I. Badawy, N. Shokri, P. Gorgojo, Flux-enhanced PVDF mixed matrix membranes incorporating APTS-functionalized graphene oxide for membrane distillation, J. Memb. Sci. 554 (2018) 309–323. doi:10.1016/j.memsci.2018.03.013.

[116] K.J. Lu, J. Zuo, T.S. Chung, Novel PVDF membranes comprising n-butylamine functionalized graphene oxide for direct contact membrane distillation, J. Memb. Sci. 539 (2017) 34–42. doi:10.1016/j.memsci.2017.05.064.

[117] Y. Li, S. Maruyama, eds., Single-Walled Carbon Nanotubes, Springer International Publishing, Cham, 2019. doi:10.1007/978-3-030-12700-8.

[118] J.K. Holt, Fast Mass Transport Through Sub-2-Nanometer Carbon Nanotubes, Science (80-. ). 312 (2006) 1034–1037. doi:10.1126/science.1126298.

[119] M. Majumder, N. Chopra, R. Andrews, B.J. Hinds, Enhanced flow in carbon nanotubes, Nature. 438

(2005) 44–44. doi:10.1038/438044a.

[120] M.S. Mauter, M. Elimelech, Environmental Applications of Carbon-Based Nanomaterials, Environ. Sci. Technol. 42 (2008) 5843–5859. doi:10.1021/es8006904.

[121] E. Balis, A. Sapalidis, G. Pilatos, E. Kouvelos, C. Athanasekou, C. Veziri, P. Boutikos, K.G. Beltsios, G. Romanos, Enhancement of vapor flux and salt rejection efficiency induced by low cost-high purity MWCNTs in upscaled PVDF and PVDF-HFP hollow fiber modules for membrane distillation, Sep. Purif. Technol. 224 (2019) 163–179. doi:10.1016/j.seppur.2019.04.067.

[122] K. Marques Lisboa, D. Busson de Moraes, C. Palma Naveira-Cotta, R. Machado Cotta, Analysis of the membrane effects on the energy efficiency of water desalination in a direct contact membrane distillation (DCMD) system with heat recovery, Appl. Therm. Eng. 182 (2021) 116063. doi:10.1016/j.applthermaleng.2020.116063.

[123] M. Khayet, T. Matsuura, Application of surface modifying macromolecules for the preparation of membranes for membrane distillation, Desalination. 158 (2003) 51–56. doi:10.1016/S0011-9164(03)00432-6.

[124] M. Qtaishat, D. Rana, M. Khayet, T. Matsuura, Preparation and characterization of novel hydrophobic/hydrophilic polyetherimide composite membranes for desalination by direct contact membrane distillation, J. Memb. Sci. 327 (2009) 264–273. doi:10.1016/j.memsci.2008.11.040.

[125] M. Essalhi, M. Khayet, Surface segregation of fluorinated modifying macromolecule for hydrophobic/hydrophilic membrane preparation and application in air gap and direct contact membrane distillation, J. Memb. Sci. 417–418 (2012) 163–173. doi:10.1016/j.memsci.2012.06.028.

[126] M. Qtaishat, M. Khayet, T. Matsuura, Guidelines for preparation of higher flux hydrophobic/hydrophilic composite membranes for membrane distillation, J. Memb. Sci. 329 (2009) 193–200. doi:10.1016/j.memsci.2008.12.041.

[127] X. Feng, L.Y. Jiang, T. Matsuura, P. Wu, Fabrication of hydrophobic/hydrophilic composite hollow fibers for DCMD: Influence of dope formulation and external coagulant, Desalination. 401 (2017) 53–63. doi:10.1016/j.desal.2016.07.026.

[128] L. Zou, P. Gusnawan, G. Zhang, J. Yu, Study of the effective thickness of the water-intrudable hydrophilic layer in dual-layer hydrophilic-hydrophobic hollow fiber membranes for direct contact membrane distillation, J. Memb. Sci. 615 (2020) 118552. doi:10.1016/j.memsci.2020.118552.

[129] D. Li, T.S. Chung, R. Wang, Morphological aspects and structure control of dual-layer asymmetric hollow fiber membranes formed by a simultaneous co-extrusion approach, J. Memb. Sci. 243 (2004) 155–175. doi:10.1016/j.memsci.2004.06.014.

[130] L. Setiawan, L. Shi, W.B. Krantz, R. Wang, Explorations of delamination and irregular structure in poly(amide-imide)-polyethersulfone dual layer hollow fiber membranes, J. Memb. Sci. 423–424 (2012) 73–84. doi:10.1016/j.memsci.2012.07.030.

[131] S.P. Sun, K.Y. Wang, N. Peng, T.A. Hatton, T.S. Chung, Novel polyamide-imide/cellulose acetate dual-layer hollow fiber membranes for nanofiltration, J. Memb. Sci. 363 (2010) 232–242. doi:10.1016/j.memsci.2010.07.038.

[132] L. Jiang, T.S. Chung, D.F. Li, C. Cao, S. Kulprathipanja, Fabrication of Matrimid/polyethersulfone dual-layer hollow fiber membranes for gas separation, J. Memb. Sci. 240 (2004) 91–103. doi:10.1016/j.memsci.2004.04.015.

[133] L.T. Duarte, C.C. Pereira, A.C. Habert, C.P. Borges, Polyurethane/polyethersulphone composite hollow fibers produced by simultaneous spinning of two polymer solutions, J. Memb. Sci. 311 (2008) 12–22. doi:10.1016/j.memsci.2007.11.030.

[134] F.Y. Li, Y. Li, T.S. Chung, H. Chen, Y.C. Jean, S. Kawi, Development and positron annihilation spectroscopy (PAS) characterization of polyamide imide (PAI)-polyethersulfone (PES) based defect-free dual-layer hollow fiber membranes with an ultrathin dense-selective layer for gas separation, J. Memb. Sci. 378 (2011) 541–550. doi:10.1016/j.memsci.2011.05.048.

[135] S. Bonyadi, T.S. Chung, R. Rajagopalan, A novel approach to fabricate macrovoid-free and highly permeable PVDF hollow fiber membranes for membrane distillation, AIChE J. 55 (2009) 828–833. doi:10.1002/aic.11688.

[136] Y. Wang, T.S. Chung, B.W. Neo, M. Gruender, Processing and engineering of pervaporation dehydration of ethylene glycol via dual-layer polybenzimidazole (PBI)/polyetherimide (PEI) membranes, J. Memb. Sci. 378 (2011) 339–350. doi:10.1016/j.memsci.2011.05.020.

[137] Y.K. Ong, T.S. Chung, Pushing the limits of high performance dual-layer hollow fiber fabricated via I2PS process in dehydration of ethanol, AIChE J. 59 (2013) 3006–3018. doi:10.1002/aic.14149.

[138] Y. Wang, S.H. Goh, T.S. Chung, P. Na, Polyamide-imide/polyetherimide dual-layer hollow fiber membranes for pervaporation dehydration of C1-C4 alcohols, J. Memb. Sci. 326 (2009) 222–233. doi:10.1016/j.memsci.2008.10.005.

[139] Q. Yang, K.Y. Wang, T.-S. Chung, Dual-Layer Hollow Fibers with Enhanced Flux As Novel Forward Osmosis Membranes for Water Production, Environ. Sci. Technol. 43 (2009) 2800–2805. doi:10.1021/es803360t.

[140] L. Setiawan, R. Wang, L. Shi, K. Li, A.G. Fane, Novel dual-layer hollow fiber membranes applied for forward osmosis process, J. Memb. Sci. 421–422 (2012) 238–246. doi:10.1016/j.memsci.2012.07.020.

[141] F.J. Fu, S. Zhang, S.P. Sun, K.Y. Wang, T.S. Chung, POSS-containing delamination-free dual-layer hollow fiber membranes for forward osmosis and osmotic power generation, J. Memb. Sci. 443 (2013) 144–155. doi:10.1016/j.memsci.2013.04.050.

[142] N. Peng, T.S. Chung, M.L. Chng, W. Aw, Evolution of ultra-thin dense-selective layer from single-layer to dual-layer hollow fibers using novel Extem® polyetherimide for gas separation, J. Memb. Sci. 360 (2010) 48–57. doi:10.1016/j.memsci.2010.04.046.

[143] X. Ding, Y. Cao, H. Zhao, L. Wang, Q. Yuan, Fabrication of high performance Matrimid/polysulfone dual-layer hollow fiber membranes for O2/N2 separation, J. Memb. Sci. 323 (2008) 352–361. doi:10.1016/j.memsci.2008.06.042.

[144] I. Ullah Khan, M.H.D. Othman, A.F. Ismail, T. Matsuura, H. Hashim, N.A.H.M. Nordin, M.A. Rahman, J. Jaafar, A. Jilani, Status and improvement of dual-layer hollow fiber membranes via co-extrusion process for gas separation: A review, J. Nat. Gas Sci. Eng. 52 (2018) 215–234. doi:10.1016/j.jngse.2018.01.043.

[145] R.A. Amaral, N.R.J.D. Mermier, A.C. Habert, C.P. Borges, Dual-layer hollow fibers for gas separation processes produced by quadruple spinning, Sep. Sci. Technol. 51 (2016) 853–861. doi:10.1080/01496395.2015.1119851.

[146] S. Pengganggu, The morphological properties study of photocatalytic TiO2/PVDF dual layer hollow fiber membrane for endocrine disrupting compounds degradation, Malaysian J. Anal. Sci. 21 (2017) 426–434. doi:10.17576/mjas-2017-2102-18.

[147] H. Dzinun, M.H.D. Othman, A.F. Ismail, M.H. Puteh, M.A. Rahman, J. Jaafar, Fabrication of Dual Layer Hollow Fibre Membranes for Photocatalytic Degradation of Organic Pollutants, Int. J. Chem. Eng. Appl. 6 (2015) 289–292. doi:10.7763/ijcea.2015.v6.499.

[148] R. Kamaludin, Z. Rasdi, M.H.D. Othman, S.H.S.A. Kadir, N.S.M. Nor, J. Khan, W.N.I.W.M. Zain, A.F. Ismail, M.A. Rahman, J. Jaafar, Visible-light active photocatalytic dual layer hollow fiber (DLHF) membrane and its potential in mitigating the detrimental effects of bisphenol A in water, Membranes (Basel). 10 (2020). doi:10.3390/membranes10020032.

[149] N. Peng, T.S. Chung, The effects of spinneret dimension and hollow fiber dimension on gas separation performance of ultra-thin defect-free Torlon® hollow fiber membranes, J. Memb. Sci. 310 (2008) 455–465. doi:10.1016/j.memsci.2007.11.018.

[150] N. Widjojo, T.S. Chung, W.B. Krantz, A morphological and structural study of Ultem/P84 copolyimide dual-layer hollow fiber membranes with delamination-free morphology, J. Memb. Sci. 294 (2007) 132–146. doi:10.1016/j.memsci.2007.02.026.

[151] D.F. Li, T.S. Chung, R. Wang, Y. Liu, Fabrication of fluoropolyimide/polyethersulfone (PES) dual-layer asymmetric hollow fiber membranes for gas separation, J. Memb. Sci. 198 (2002) 211–223. doi:10.1016/S0376-7388(01)00658-5.

[152] R.A. Amaral, C.P. Borges, A.C. Habert, N.R.J.D. Mermier, Dual-Layer Hollow Fibers for Sulfur Removal from Fuels, Chem. Eng. Technol. 39 (2016) 1171–1176. doi:10.1002/ceat.201500272.

[153] X. Ding, Y. Cao, H. Zhao, L. Wang, Interfacial morphology between the two layers of the dual-layer asymmetric hollow fiber membranes fabricated by co-extrusion and dry-jet wet-spinning phase-inversion techniques, J. Memb. Sci. 444 (2013) 482–492. doi:10.1016/j.memsci.2013.03.035.

[154] L.Y. Jiang, H. Chen, Y.-C. Jean, T.-S. Chung, Ultrathin polymeric interpenetration network with

separation performance approaching ceramic membranes for biofuel, AIChE J. 55 (2009) 75–86. doi:10.1002/aic.11652.

[155] J. Zuo, T.S. Chung, G.S. O'Brien, W. Kosar, Hydrophobic/hydrophilic PVDF/Ultem® dual-layer hollow fiber membranes with enhanced mechanical properties for vacuum membrane distillation, J. Memb. Sci. 523 (2017) 103–110. doi:10.1016/j.memsci.2016.09.030.

[156] D. Bhandari, K.O. Olanrewaju, N. Bessho, V. Breedveld, W.J. Koros, Dual layer hollow fiber sorbents: Concept, fabrication and characterization, Sep. Purif. Technol. 104 (2013) 68–80. doi:10.1016/j.seppur.2012.11.003.

[157] S. Bonyadi, T.S. Chung, Flux enhancement in membrane distillation by fabrication of dual layer hydrophilic-hydrophobic hollow fiber membranes, J. Memb. Sci. 306 (2007) 134–146. doi:10.1016/j.memsci.2007.08.034.

[158] F. Edwie, M.M. Teoh, T.S. Chung, Effects of additives on dual-layer hydrophobic-hydrophilic PVDF hollow fiber membranes for membrane distillation and continuous performance, Chem. Eng. Sci. 68 (2012) 567–578. doi:10.1016/j.ces.2011.10.024.

[159] M.M. Teoh, T.S. Chung, Y.S. Yeo, Dual-layer PVDF/PTFE composite hollow fibers with a thin macrovoid-free selective layer for water production via membrane distillation, Chem. Eng. J. 171 (2011) 684–691. doi:10.1016/j.cej.2011.05.020.

[160] J. Zhu, L. Jiang, T. Matsuura, New insights into fabrication of hydrophobic/hydrophilic composite hollow fibers for direct contact membrane distillation, Chem. Eng. Sci. 137 (2015) 79–90. doi:10.1016/j.ces.2015.05.064.

[161] H. Dzinun, M.H.D. Othman, A.F. Ismail, M.H. Puteh, M.A. Rahman, J. Jaafar, Morphological study of co-extruded dual-layer hollow fiber membranes incorporated with different TiO2 loadings, J. Memb. Sci. 479 (2015) 123–131. doi:10.1016/j.memsci.2014.12.052.

[162] A.L. Ahmad, W.K.W. Ramli, Hydrophobic PVDF membrane via two-stage soft coagulation bath system for Membrane Gas Absorption of CO2, Sep. Purif. Technol. 103 (2013) 230–240. doi:10.1016/j.seppur.2012.10.032.

[163] S.P. Sun, T.A. Hatton, S.Y. Chan, T.S. Chung, Novel thin-film composite nanofiltration hollow fiber membranes with double repulsion for effective removal of emerging organic matters from water, J. Memb. Sci. 401–402 (2012) 152–162. doi:10.1016/j.memsci.2012.01.046.

[164] M.A. Usmani, I. Khan, N. Ahmad, A.H. Bhat, D.K. Sharma, J.A. Rather, S.I. Hassan, Modification of Nanoclay Systems: An Approach to Explore Various Applications, in: Nanoclay Reinf. Polym. Compos. (Pp. 329-356). Springer, Singapore., 2016: pp. 57–83. doi:10.1007/978-981-10-1953-1_3.

[165] M. Su, M.M. Teoh, K.Y. Wang, J. Su, T.S. Chung, Effect of inner-layer thermal conductivity on flux enhancement of dual-layer hollow fiber membranes in direct contact membrane distillation, J. Memb. Sci. 364 (2010) 278–289. doi:10.1016/j.memsci.2010.08.028.

[166] M. Pagliero, A. Bottino, A. Comite, C. Costa, Silanization of tubular ceramic membranes for application in membrane distillation, J. Memb. Sci. 601 (2020) 117911. doi:10.1016/j.memsci.2020.117911.

[167] W. Zhang, Y. Li, J. Liu, B. Li, S. Wang, Fabrication of hierarchical poly (vinylidene fluoride) micro/nano-composite membrane with anti-fouling property for membrane distillation, J. Memb. Sci. 535 (2017) 258–267. doi:10.1016/J.MEMSCI.2017.04.051.

[168] P. Wang, M.M. Teoh, T.S. Chung, Morphological architecture of dual-layer hollow fiber for membrane distillation with higher desalination performance, Water Res. 45 (2011) 5489–5500. doi:10.1016/j.watres.2011.08.012.

[169] L. Zhao, C. Wu, Z. Liu, Q. Zhang, X. Lu, Highly porous PVDF hollow fiber membranes for VMD application by applying a simultaneous co-extrusion spinning process, J. Memb. Sci. 505 (2016) 82–91. doi:10.1016/j.memsci.2016.01.014.

[170] N. Li, C. Xiao, S. An, X. Hu, Preparation and properties of PVDF/PVA hollow fiber membranes, Desalination. 250 (2010) 530–537. doi:10.1016/j.desal.2008.10.027.

[171] Y. Xiuli, C. Hongbin, W. Xiu, Y. Yongxin, Morphology and properties of hollow-fiber membrane made by PAN mixing with small amount of PVDF, J. Memb. Sci. 146 (1998) 179–184. doi:10.1016/S0376-7388(98)00107-0.

[172] A. Anvari, A.A. Yancheshme, F. Rekaabdar, M. Hemmati, M. Tavakolmoghadam, A. Safekordi, PVDF/PAN Blend Membrane: Preparation, Characterization and Fouling Analysis, J. Polym. Environ. 25 (2017) 1348–1358. doi:10.1007/s10924-016-0889-x.

[173] F. Edwie, T.S. Chung, Development of hollow fiber membranes for water and salt recovery from highly concentrated brine via direct contact membrane distillation and crystallization, J. Memb. Sci. 421–422 (2012) 111–123. doi:10.1016/j.memsci.2012.07.001.

[174] H. Strathmann, Preparation of Microporous Membranes by Phase Inversion Processes BT - Membranes and Membrane Processes, in: E. Drioli, M. Nakagaki (Eds.), Springer US, Boston, MA, 1986: pp. 115–135. doi:10.1007/978-1-4899-2019-5_13.

[175] I.M. Wienk, R.M. Boom, M.A.M. Beerlage, A.M.W. Bulte, C.A. Smolders, H. Strathmann, Recent advances in the formation of phase inversion membranes made from amorphous or semi-crystalline polymers, in: J. Memb. Sci., Elsevier Science B.V., 1996: pp. 361–371. doi:10.1016/0376-7388(95)00256-1.

[176] X.H. Cao, M. Qiu, A.W. Qin, C.J. He, H.F. Wang, Effect of additive on the performance of PVDF membrane via non-solvent induced phase separation, Mater. Sci. Forum. 789 (2014) 240–248. doi:10.4028/www.scientific.net/MSF.789.240.

[177] N. Peng, T.S. Chung, K.Y. Wang, Macrovoid evolution and critical factors to form macrovoid-free hollow fiber membranes, J. Memb. Sci. 318 (2008) 363–372. doi:10.1016/j.memsci.2008.02.063.

[178] M. Bahrami, J. Karimi-Sabet, A. Hatamnejad, A. Dastbaz, M.A. Moosavian, Optimization and

modification of PVDF dual-layer hollow fiber membrane for direct contact membrane distillation; application of response surface methodology and morphology study, Korean J. Chem. Eng. 35 (2018) 2241–2255. doi:10.1007/s11814-018-0038-4.